UNIVERSITÉ DU QUÉBEC

MÉMOIRE PRÉSENTÉ À
L'UNIVERSITÉ DU QUÉBEC À CHICOUTIMI
COMME EXIGENCE PARTIELLE
DE LA MAÎTRISE EN INGÉNIERIE

Par

Sona Maralbashi-Zamini

Developing Neural Network Models to Predict Ice Accretion Type and Rate on Overhead Transmission Lines

Développement de réseaux de neurone pour la prédiction du type et du taux de glace accumulée sur les lignes aériennes de transport d'énergie électrique

August 2007

Mise en garde/Advice

Abstract:

A large number of overhead transmission lines are exposed to atmospheric icing in remote northern regions. Appropriate icing models to estimate transmission line icing are critical for companies to optimize the design of reliable equipment able to operate in this environment. For electricity companies, ice load forecasting can help determine the operational impacts on their equipment so that serious damage can be avoided.

The present research carried out within the framework of the Industrial Chair CRSNG/Hydro-Quebec/UQAC on atmospheric icing of power network equipment (CIGELE), focuses on: (i) The development of models to predict accreted ice type on exposed structures and (ii) development of empirical models to predict ice accretion rate on transmission lines.

Initially, with the purpose of developing neural network models for determining accreted ice type, a training data set was created, based on functions extracted from the International Electrotechnical Commission (IEC) reference which relates ice type to temperature and wind speed variables. The Multi Layer Perceptron (MLP) architecture of neural networks was selected as the experimented architecture and its different characteristics were tested in order to find the optimum design. The initial two-input model was improved by incorporation of an additional parameter, a droplet size variable. Developed models have a correct prediction of 100% with the training data set and more than 99% correct prediction with a test data set. The results obtained are promising and show that neural network models can be a good alternative for predicting ice type, provided that the functions used for creating training data sets are accurate enough.

In the second part of this study, three models were developed in order to predict ice accretion rate on the transmission lines in corresponding situations. The data used for developing these models come from the Mont Bélair measuring station which is part of Hydro-Quebec's SYGIVRE real-time network. The first model was developed by being trained with data of three phases of an icing event, including accretion, persistence, and shedding. The second model was developed for wet icing which was trained by events which had been occurring during precipitations. Finally, the third model was developed by being trained with only the accretion phase of an icing event. In developing these models, four architectures of neural networks, including one-hidden layer MLP, two-hidden layers MLP, and Elman and Jordan's recurring network as well as more than two hundred different configurations for each architecture were tested and compared. Also, for each configuration, two learning styles including batch and incremental styles were tested. The number of inputs taken from previous time steps was another parameter that was varied in order to determine the optimum design.

As a general conclusion, Jordan's recurrent neural network with inputs taken from three previous time steps was the architecture which gave the best results with all three models. The main characteristics and advantage of this architecture were that it uses the estimated quantities of ice accretion in the past to estimate the current ice accretion. So, this network is characterized by recurrent loops. In the case of the comparison between efficiency of these three predictive models, it was observed that the model developed by making use of the most homogenous data, i.e., only ice accretion phase, is the best among these three models as it can generalize very well and closely estimate extreme ice loads. The performance of the developed models demonstrates that the models developed with

Jordan's architecture of neural networks make an important contribution in the development of accurate empirical models for estimating power transmission line icing loads, provided that a reasonable number of training data points are used and the data going into the networks are carefully chosen.

Résumé:

Un grand nombre de lignes aériennes de transport d'énergie électrique sont exposées à la glace atmosphérique dans les régions nordiques éloignées. Des modèles appropriés pour estimer les quantités de glaces sur les lignes de transport s'avèrent très précieux pour aboutir à la conception d'équipement fiable capable d'opérer dans cet environnement. Pour les compagnies d'"électricité, les prédictions de charge de glace peuvent aider à déterminer les impacts opérationnels sur leur équipement, de sorte que des dommages sérieux puissent être évités.

La présente recherche, effectuée dans le cadre des travaux de la Chaire industrielle CRSNG/HYDRO-QUÉBEC/UQAC sur le givrage atmosphérique des équipements des réseaux électriques (CIGELE), se concentre sur : (i) le développement des modèles pour prédire le type de glace accumulé sur les structures exposées et (ii) le développement des modèles empiriques pour prédire le taux d'augmentation de glace sur des lignes de transport.

Dans le but de réaliser une classification de type de glace en utilisant les réseaux de neurones, un ensemble de données a été créé en se basant sur des fonctions extraites à partir de la référence de la Commission Électrotechnique Internationale (CEI) qui relie le type de glace aux variables de la température et de la vitesse de vent. Le réseau Perceptron multicouches (MLP) a été utilisé et différentes caractéristiques ont été examinées afin de trouver l'architecture optimale. Ce modèle initial de deux entrées a été amélioré en ajoutant un troisième paramètre qui est la taille des gouttelettes. Les modèles développés donnent un taux de reconnaissance de 100% avec les données d'entraînement et plus de 99% avec les données de test. Les résultats obtenus sont prometteurs et

prouvent que les modèles basés sur les réseaux de neurones peuvent être une bonne alternative pour la classification de type de glace à condition que les fonctions utilisées pour générer les données d'entraînement soient assez précises.

Dans la deuxième partie de cette étude, trois modèles ont été développés afin de prédire le taux d'augmentation de glace sur les lignes de transport dans des situations correspondantes. Les données utilisées pour entraîner les réseaux de neurones proviennent du site du Mont Bélair qui fait partie du système de surveillance en temps réel SYGIVRE d'Hydro-Québec. Le premier modèle neural a été entraîné avec les données des trois phases d'un événement de givrage, soit la phase d'accrétion, la phase de persistance et la phase de délestage. Le deuxième modèle a été développé pour le givrage humide et a été entraîné avec les trois phases des événements produits pendant les précipitations. Finalement, le troisième modèle développé a été entraîné avec seulement la phase d'accrétion d'un événement de givrage. Pour établir ces modèles, quatre architectures de réseaux de neurones comprenant MLP avec une couche cachée, MLP avec deux couches cachées, le réseau récurrent Elman et Jordan ainsi que deux cents différentes configurations pour chaque architecture ont été examinées et comparées. En outre, pour chaque configuration, deux styles d'entraînement soit par batch ou incrémental ont été examinés. Le nombre d'entrées prises des incréments de temps antérieurs, est un autre paramètre qui a été étudié afin de déterminer la conception optimale.

Comme conclusion générale, le réseau récurrent Jordan avec un délai de trois unités était la meilleure architecture et ceci pour les trois modèles. Les caractéristiques et l'avantage principaux de cette architecture donnant les meilleurs résultats, c'est qu'elle

utilise les quantités de glace estimée dans le passé pour estimer celle en cours. Donc, le réseau en question se caractérise par une boucle récurrente. Dans le cas de la comparaison entre l'efficacité de ces trois modèles prédictifs, on a observé que le modèle développé en se servant des données les plus homogènes, c'est-à-dire seulement les données de la phase d'accrétion de glace, est le meilleur parmi ces trois modèles puisqu'il peut généraliser et estimer étroitement les charges de glace extrême. La performance des modèles développés démontre que les modèles établis avec l'architecture Jordan de réseaux de neurones peuvent apporter une contribution importante dans le développement des modèles empiriques précis pour estimer les charges de glace des lignes de transport d'énergie, à condition qu'un nombre raisonnable de données d'entraînement soit utilisé et que les données allant aux réseaux soient soigneusement choisies.

Dedicated to:

My loving and supportive family:

My dear husband, Hossein

My beloved parents, Ata and Ana

&

My lovely sisters and brother, Sevda, Dourna, and Samad

Acknowledgments:

Table of Contents

Chapter 6

List of Figures

List of Tables

Abbreviations and Symbols

ANN   *Artificial Neural Network*

CIGELE   *The Industrial Chair on Atmospheric Icing of Power Network Equipment*

FFNN   *Feedforward Neural Network*

INGIVRE   *Canada Research Chair on Engineering of Power Network Atmospheric Icing*

IRM   *Icing-Rate-Meter*

LRP   *Learning Rate Percentage*

MLP   *Multi Layer Perceptron*

MSE   *Mean-Square-Error*

NMSE   *Normalized Mean Square Error*

PE   *Processing Element*

RNN   *Recurrent Neural Network*

$\hat{I}$ *Predicted ice accretion rate*

D   *Droplet size*

I   *Ice accretion rate*

P   *Precipitation rate*

S   *Number of IRM Signals*

T   *Temperature*

t   *Time step*

W   *Wind speed*

Z   *Wind direction*

Chapter 1

General Introduction

Chapter 1

General Introduction

1.1 Background

Atmospheric icing of structures affecting overhead electrical power networks is a phenomenon that takes place very frequently in cold regions of the world such as Canada, France, Norway and some other cold-climate countries. In these regions, power transmission lines need to travel through vast areas exposed to the atmosphere before servicing the population. Normal operation of electric power systems will be endangered by the accumulation of ice in the transmission lines which may result in the power disruption and subsequent disruption of community services and daily life. Reducing the effects of atmospheric icing is not easy because dimensioning the structures to undergo heavier ice loads rapidly increases construction costs. Accordingly, in order to optimize the design of power transmission line structures, it is very important to have estimates for the rates of ice load by developing reliable ice accretion models to be able to forecast ice loads as accurately as possible [5] [35] [41].

1.2 Research Problem

Ice accretion is a major problem for a number of industries, such as electric power systems, aerospace and so forth. However, this study is concerned only with electric power systems. There are two main negative effects of accumulated ice or snow on electrical equipments [35]. The first is excessive mechanical loading of towers, transmission lines and substation hardware; this can lead to either deceleration or

2

temporary stops in proper operation of apparatus or, in extreme cases, to major collapsing of the lines with dramatic consequences. The second is a change in the insulation performance of insulating material and structures that may sometimes result in flashover faults and the consequent power outages. Such events have been reported by many researchers in several countries [2] [16][28].

In Canada, as in other cold countries, ice accumulation coupled with wind has caused significant damages to electric power systems. In January 1998, billions of dollars worth of damage was caused to electrical equipment in eastern Canada during the "Great Ice Storm" [14]. A sequence of three ice storms hit, in quick succession, the areas of southern and western Quebec, eastern Ontario and part of the Atlantic provinces. Over the period of January 5-9, about 100 mm of freezing rain fell on these regions. Ice accretion resulted in the collapse of more than 1,000 power transmission steel towers (including 735 kV level towers), and 30,000 wooden poles.

Because of the aforementioned problems, a lot of studies have been conducted in order to understand the physical process involved during ice accretion on structures. According to Poots [48], three main methods of investigation have been employed:

1. *Continuous field measurements of ice load and wind-on-ice load allied with the simultaneous measurement of meteorological variables;*
2. *Simulations using an icing wind tunnel;*
3. *Construction of mathematical /computational icing models.*

Of these methods, the most reliable one is the study based on the field data. The development of communication technologies and information processing systems has enabled electricity companies to monitor the loads on transport lines in a real-time manner, a practical way to reduce the risks of ice accumulations and also to develop their databases for snow and ice load measurements on overhead transmission line conductors. Such field data bases are also fundamental in the validation of experimental and theoretical simulation of the icing process. One electricity company always concerned with furnishing the proper field data is Hydro-Quebec, which began monitoring the transport lines throughout the province of Quebec three decades ago. In this regard, two icing measurement networks (PIM and SYGIVRE) have been created to collect data from measuring sites and save it into databases.

Because of the importance of ice accretion modeling based on field data, the Industrial Chair on Atmospheric Icing of Power Network Equipment (CIGELE) has "*processing data from natural sites and probabilistic model elaboration*" as one of its important research categories. The present work fits in this category and aims to analyze the data collected from one of the monitoring stations of the SYGIVRE network and develop a model with better capability of predicting ice accumulation on transport lines.

Processing data from natural sites has generally been done using statistical approaches. However, newly-developed technology and calculation methods make it possible and necessary to develop new ice models capable of better satisfying the needs of the people involved, both in terms of performance and accessibility of models.

4

Although, a number of valuable investigations for predicting ice accumulation have been carried out, to the best of our knowledge there has been no detailed and systematic study using one of the new technologies in this field (artificial neural networks) and a review of literature revealed the necessity for further analysis and improvements in the previous models.

1.3 Objectives

This study pursues two main objectives:

Developing neural network models to predict the type of accreted ice is the first objective of this study. Given meteorological parameters, the models are intended to determine the type of accreted ice.

Developing neural network models to forecast the hourly ice accretion rate on the overhead transmission lines is the second objective. To achieve optimum models, different architectures of neural networks together with different configurations for each of the architectures will be studied. Also, by filtering the available data according to different criteria, the utility of distinctive models in the prediction of accreted ice will be studied. All models will be developed using real icing events which occurred at the Mont Bélair measuring station and recorded by the SYGIVRE network of Hydro-Quebec.

1.4 Methodology

This research work was realized in two parts, each of which addresses one of the aforementioned objectives. The steps taken in the first part in order to obtain predictive models for determining type of accreted ice are as follows:

1. Studying available methods of determining ice type and creating training data sets using these methods

2. Developing neural network models to determine ice type based on the created data sets

Similarly, the steps taken in the second part of this study in order to obtain models for predicting accreted ice rate are:

1. Analyzing and describing the available data of icing events which have occurred in the Mont Bélair station

2. Carrying out a series of initial experiments in now casting mood, considering only the accretion phase of icing events in order to find candidates for developing predictive models

3. Filtering the database and developing separate predictive models corresponding to each filtered data

1.5 Overview of the Thesis

This thesis is presented in six chapters. After a general introduction in Chapter 1, a review of the methods used in literature for predicting ice accretion on exposed structures will be presented in Chapter 2. Since neural networks play a central role in this research, Chapter 3 will provide some insights in the area of neural networks, covering architectures used in the rest of the thesis. In Chapter 4, a novel neural network approach for predicting accreted ice type will be introduced. Chapter 5 begins with a preliminary analysis and a description of the available icing data base and includes the experimented architectures of neural networks for predicting ice accretion on exposed structures. Finally, in Chapter 6, some general conclusions are summarized from analyses and discussions of the results reported in the previous chapters. In addition, some recommendations are provided for future research.

Chapter 2

Literature Review

Chapter 2

Literature Review

2.1 Introduction to ice accretion models

The term ice accretion or icing is used to describe the process of ice increase on a surface exposed to the atmosphere. In the past years, there has been considerable research activity in the study of the icing of structures with generally two orientations, including icing of transmission lines and telecommunication towers. Studies have been conducted independently in different countries such as Canada, Japan, Iceland, Britain, Czech Republic, Finland, France, Germany, Hungary, Iceland, Norway, Russia, Switzerland, and the United States [48]. Through this research activity, much progress has been made in understanding the atmospheric icing phenomena. The three commonly-used methods in conducting these researches include:

1. Mathematical or computational modeling
2. Modeling based on the simulations using an icing wind tunnel
3. Modeling based on field measurements

The details of these methods will be elaborated on in the following sections.

2.2 Mathematical or computational modeling

Mathematical or computational modeling is based on the known physics of the accretion process. There are various models used in practical and theoretical studies today. Some models have focused on the effect of an average freezing rain intensity on a simplified shape, which in most cases is a circular cylindrical accretion shape, whereas

detailed models simulate the formation of the accretion shape based on detailed drop trajectories and heat transfer, expressed as conservation of momentum, energy and mass equations under specified boundary and initial conditions [5][6].

2.2.1 Analytical modeling

These models have been used to make estimations of ice intensity employing concepts of heat and mass transfer and continuum mechanics under boundary or initial conditions [48]. They are called continuous because they are based on the assumption of continuous changes of all the physical parameters. Two of the commonly-used analytical models for freezing rain precipitation are that of Imai and Chainé and Castonguay.

Imai's model [26] was based on the idea that the icing intensity is controlled by the heat transfer from the cylinder, i.e. the icing mode is wet growth. He proposed that the growth rate of glaze per unit length of cable is:

$$\frac{dM}{dt} = C_1 \sqrt{VR}\,(-T) \qquad\qquad 2\text{-}1$$

where M is the glaze weight per meter, V is the wind speed, R is the radius of the iced cylinder, T is the temperature, and C_1 is a constant. Integrating Equation 2-1 gives:

$$R^{3/2} = C_2 \sqrt{V}\,(-T)t \qquad\qquad 2\text{-}2$$

where a fixed value (of 0.9 g cm^{-3}) is assumed for the ice density and t is the time. In this simple model dM/dt is proportional to $-T$ and the precipitation intensity I has no effect. Although the model is conceptually correct, it was shown that it overestimates ice loads under typical conditions where water flux rather than the heat transfer controls icing.

Also, the model underestimates ice loads in extreme conditions because the value of C_2 is too small.

Instead of assuming a cylindrical accretion shape, Chainé and Castonguay [4] developed a model that assumes a semi-elliptical accretion shape on one side of the cable. In such a case, the cross-sectional area of the ice deposit S_i becomes:

$$S_i = \frac{\pi R_0}{2}\sqrt{H_g^2 + H_v^2}$$

2-3

where H_v is the thickness of the water layer deposited on a vertical surface, H_g is the depth of liquid precipitation, and R_0 is the radius of the cable. They then define a correction factor K as the ratio of the real cross-sectional area and the one calculated from Equation 2-3. This correction factor was determined empirically from the marine icing wind-tunnel experiments of Stallabrass and Hearty [55] as a function of R_0 and air temperature τ_a. Comparing S_i with the radial ice section, Chainé and Castonguay show that the equivalent radial ice thickness is:

$$\Delta R = \left[\frac{R_0 K}{2}\sqrt{H_g^2 + H_v^2} + R_0^2\right]^{1/2} - R_0$$

2-4

This model shows a strong dependence of radial equivalent ice thickness on cable diameter.

2.2.2 Numerical modeling

By development of technology and calculation methods, many numerical models have been realized to simulate ice accretion on transmission lines and cables. The main advantage of numerical modeling is that the time-dependent effects can be included and,

therefore, changes in the input parameters can be easily taken into consideration. Furthermore, these models can simulate both regimes of ice growth, i.e., wet growth (glaze ice) and dry growth (rime icing) by using heat balance calculations. Thus, these models don't need any pre-assumptions of the icing mode [37].

Amongst the earlier work on the numerical modeling is the research of Makkonen [38]. Makkonen [38] presented a time-dependent numerical model of icing on wires which handles the icing wire as a growing, slowly rotating circular cylinder. According to this model, the icing intensity on a circular cylinder is:

$$I = \frac{2}{\pi} Envw$$ 2-5

where E is the collection coefficient which was calculated based on the numerical solution of Langmuir and Blodgett [32] , n is the freezing fraction which is calculated from the heat balance of the icing surface, v is the wind speed, and w is the liquid water content in the air. Ice growth is considered wet when $n<1$ and it is considered dry when $n=1$.

During the ice accretion process on a structure, the diameter of the icing object changes, and therefore E and n depend on time τ. When the atmospheric conditions are kept unchanged, it follows from Equation 2-5 that the ice load M_i per unit length of the wire at time τ_i is:

$$M_i = \int_0^{\tau_i} I(\tau)\frac{\pi}{2}D(\tau)d\tau = vw \int_0^{\tau_i} E(\tau)n(\tau)D(\tau)d\tau$$ 2-6

In this model, the calculations of the ice load M_i are made in a step-wise manner. For each time-step i, the collection coefficient E_i is calculated and the freezing fraction n_i is determined. Then the icing intensity I_i is obtained from Equation 2-5, and the ice load M_i is:

$$M_i = M_{i-1} + I_{i-1} \frac{\pi}{2} D_{i-1} \Delta\tau \qquad\qquad 2\text{-}7$$

This model was improved in [37] so that the direct water impingement on the growing icicles can be taken into consideration and simulate spongy ice growth.

2.2.3   Stochastic modeling

Analytical continuous models that are based on differential forms of the equations for the conservation of momentum, energy, and mass have the limitation of providing reasonable results only when the initial shape does not undergo substantial alteration. The most demanding cases occur when the accretion is very wet and has a complex geometry which changes with time [58] . As an alternative to the continuous models, Monte Carlo models have been used in ice accretion research. In this method, the motion of each drop or of drop ensembles is examined directly. This approach has been applied successfully to predict accretion under riming conditions when impinging small droplets freeze on impact. For example, Gates et al., [20] studied accretion on a fixed cylinder and Personne et al., [47] carried out a similar investigation on a rotating cylinder.

In 1993, Szilder [57] introduced a random walk method into ice accretion research that includes empirically-based freezing probability and shedding parameters. The

random walk model builds up an ice accretion structure using discrete elements or particles. By developing this new approach, Szilder carried out a two-dimensional [56] and three-dimensional [59] analysis of the ice accretion on a cylinder. These models are a combination of a ballistic trajectory and a random walk model. A ballistic model determines the location of impact of the fluid element, and the behavior of the fluid element flowing along the surface is predicted by a random walk process.

The main advantages of a random walk model are that they allow the efficient representation of water flow along an accretion and fluid particles can move considerably away from the location of the initial impact. Also, the random walk model adds some randomness to accretion shapes which results in a very good concordance with experimental observation. However, one difficulty with this approach is the verification of their simulations.

2.3   Modeling based on simulations using an icing wind tunnel

The advantage of this method for studying ice and snow accretion is that the effects of changes in flow and thermal conditions on the accretion process can be readily assessed and analyzed. However, the main drawback is that achieving a one-to-one correspondence between the icing wind tunnel and field conditions is very difficult because there are many physical and meteorological variables, i.e., flow and thermal parameters controlling an accretion process [48]. One of the empirically achieved equations for modeling freezing rain accretion is Lenhard's [34] model. Using empirical data, Lenhard [34] proposed that the ice weight per meter M is:

$$M = C_3 + C_4 H_g \qquad\qquad 2\text{-}8$$

where H_g is the total amount of precipitation during the icing event and C_3 and C_4 are constants. It follows from Equation 2-8 that:

$$\frac{dM}{dt} = C_4 I \qquad\qquad 2\text{-}9$$

where I is the precipitation intensity. According to Makkonen [37], this model is very simplistic because it neglects all effects of wind and air temperature.

2.4 Empirical modeling based on field measurements

In spite of important progress in the development of mathematical or empirical icing models, there still is no perfect model which can describe the evolution of atmospheric icing. This is mainly related to:(i) the complication of the ice accumulation phenomenon itself, which results from complex interactions between materials and fluids and involves atmosphere dynamics which are difficult to model and predict and (ii), the difficulty in assessing the relevant input parameters e.g., liquid water content and droplet sizes, because of the considerable technical problems involved in measuring these quantities accurately, even under laboratory conditions [38][41]. These problems force the researchers to simplify assumptions that consequently restrict the models that are developed.

As an alternative method, modeling based on the field measurements seems to be more realistic and promising. The objective of this approach is to find a correlation

between the meteorological conditions, measuring instrument materials, and the corresponding ice load on the transmission lines. In this perspective and in order to meet the growing demands of furthering the knowledge about the atmospheric icing, electricity companies have begun to develop their databases for snow and ice load measurements on overhead transmission line conductors in the past three decades [48]. Such icing databases began to exist in Quebec in 1974 when Hydro-Quebec installed its first monitoring system, a network with over 170 Passive Ice Meters (PIM) , deployed throughout the province. Later, in 1992, thanks to the developments in communication technology, Hydro-Quebec installed a new monitoring system that, contrary to the previous network, was active in the sense that its measuring devices are automatic. This network is called SYGIVRE and includes more than 30 measuring stations equipped with Icing Rate Meters (IRM), the automatic measuring device [17].

The exploration of the historical meteorological data of the available icing databases has enabled the researchers to conduct studies in several directions such as investigating the return period for extreme freezing rain icing events [29][30][36], analysis of spatial and temporal distribution of icing events [8][12][21][24], creating models for detecting the occurrence of ice storms [15][39] and developing models for estimating ice load on transmission lines [18][41][46][52][50][52][54]. In the domain of modeling ice accretion based on field measurements, two approaches have been taken by the researchers. These include the statistical approach using multi-variable regression and the neural network approach.

2.4.1 Statistical models

Numerous investigations have been reported by the researchers and aim at estimating actual ice accretion on overhead transmission lines using icing databases and statistical tools. A brief description of some of these works follows.

A model was obtained by McComber et al. [42] by using multi-variable linear regression which relates instrumentation readings to measured cable load. This approach is the simplest model within the empirical modeling of ice accretion. Savadjiev et al. [54] studied the estimation of ice accretion weight by converting the measured tension force of transmission cables into linear ice mass using data from two icing test sites in Quebec (Mt. Bélair and Mt. Valin).

The probabilistic distribution of the icing rate and meteorological parameters was another study carried out by Savadjiev et al. [53]. In order to establish quantitative relations and a theoretical basis for the creation of a probabilistic model of icing, the icing events were classified according to the process of icing growth, in-cloud icing and precipitation icing (freezing rain). The one-dimensional analysis performed in these studies can be considered the first stages toward establishing a working probability-based model for studying icing process.

In another valuable study, Farzaneh et al. [18] established a numerical model which calculated hourly icing rate as a function of the number of IRM signals, ambient temperature, wind speed and direction, and precipitation rate. This study considered only

the precipitation icing events because these events have important influence on the mechanical reliability of the overhead power lines.

2.4.2   Neural network models

Within the empirical modeling, neural networks offer a new approach for modeling transmission line icing. Following the success of applying neural networks in different fields, there has been great interest in using neural network techniques for predicting atmospheric icing in recent studies. This interest is mainly because of the utility of neural network models in inferring a function from observations. This is particularly useful in applications where the complexity of the data or task makes the design of such a function by hand impractical, which is the case with icing data. The neural network approach uses directly measured data to train the model, i.e., to optimize its parameters, so that the model gives the right answer to the input variables.

The first neural network model, developed in Japan [46], was an on-line warning system to detect disasters caused by ice accretion on power lines. The input parameters of this model were temperature, precipitation intensity, and wind velocity. The binary output represented disaster in the case of 1 and no disaster in the case of 0. Because a large-scale database was used in this study, the system was very useful.

Following the same idea, another model was developed for estimating ice accretion load on transmission line structure [41]. This model was developed using data from the Mont Bélair icing site and it used as inputs four parameters: temperature, precipitation

rate, IRM signals, and normal wind speed. The model was trained using data of the accretion phase of an icing event. Different characteristics of the feedforward neural network with time delays were tested and it was concluded that a one-hidden layer with 9 neurons in the hidden layer yields the best results.

The results of these models motivated deeper research work which was carried out by Larouche et al. [33]. This study explored five different architectures of neural network in order to find the architecture which is most appropriate for the task of ice accretion prediction. Two static networks, Multilayer Perceptron and Radial Basis Functions, as well as two time dependent networks, Finite Impulse Response (FIR) and Elman, were studied and compared. This study was also based on the data taken from the Mont Bélair icing site. The neural networks in this study make use of the following input variables: temperature, normal wind speed, and IRM signals. The load cell signal constitutes the output variable. The results indicated that the FIR network yielded the best prediction.

The neural network approach to ice accretion modelling has the advantage of adapting the model to new data as they become available; it means that the training can be done repeatedly. This is considered an advantage because rapid progress in instrumentation and telecommunication enables the companies involved to collect more and more icing data. In this context, neural networks appear to be a promising technique of artificial intelligence which can make an important contribution in the development of an accurate empirical model for estimating power transmission line icing loads.

2.5 Insertion of the present work

The present work fits in the second category of empirical modeling and aims at adapting the most adequate neural network architecture to the prediction of ice accretion. Neural network is a fairly new technique, at least as applied to transmission line icing, and it offers a vast number of different configurations and possibilities. Hence, it remains possible to improve the previously-achieved models by changing the network design characteristics. Furthermore, it is possible to improve the neural systems further by filtering input data. The neural networks discussed above were trained by applying all available data. However, the physics of in-cloud icing and precipitation icing (freezing rain) is different enough to justify a division of the data in two groups corresponding to the appropriate situation. In this perspective, the present work aims to be an extension of the previous neural models by considering further configurations of networks and by applying more discrimination on the input data.

2.6 Summary

In this chapter, different methods used for modeling ice accretion on transmission lines have been reviewed. The chapter begins with a brief description of mathematical modeling and modeling based on simulation using a wind tunnel. Then, two approaches of empirical modeling, based on field measurements including statistical and neural network techniques, have been presented. At the end of the chapter, the motivations for carrying on the present work which fits into the neural network approach have been discussed.

Chapter 3
Neural Networks

Chapter 3

Neural Networks

3.1 Introduction

Neural networks, more precisely called Artificial Neural Networks (ANN), are computational models consisting of a number of simple processing elements (PEs) that communicate by sending signals to each other over a large number of weighted connections. The original inspiration for neural networks comes from the discovery that complex learning systems in the brain of animals consist of sets of highly interconnected neurons [9]. A biological neuron collects signals from other neurons through a host of fine structures called dendrites. The neuron sends out spikes of electrical activity through a long, thin strand known as an axon, which splits into thousands of branches. At the end of each branch, a structure called a synapse converts the activity from the axon into electrical effects that inhibit or excite activity in the connected neurons. When a neuron receives excitatory input that is sufficiently large compared to its inhibitory input, it sends a spike of electrical activity down its axon. Learning occurs by changing the effectiveness of the synapses so that the influence of one neuron on another changes [7]. Although the structure of a given neuron can be very simple, the networks of densely interconnected neurons can solve complex tasks such as the classification and the recognition of patterns. For example, the human brain contains approximately 10^{11} neurons, each of which is connected on average to 10,000 other neurons, making a total of 10^{15} synaptic connections. The ANNs represent an attempt on a very basic level to imitate the type of nonlinear training which occurs in the neural networks that we find in nature. In fact, the

relationship between an ANN and the brain lies in the idea of performing computations by using parallel interaction of a very large number of PEs.

Neural networks have been used in connection with many different applications. The tasks to which they are applied tend to fall within two broad categories: problems of pattern recognition/classification and function approximation. Typically, a network will be asked to classify an input pattern as belonging to one of a number of different possible classes, or to produce an output value of one or more input values. This is done by representing the system with a representative set of examples describing the problem, namely pairs of input and output samples; the network will then be trained to infer the mapping between input and output data. This ability to learn how to make the desired mapping from inputs to outputs without explicitly having to be told the rules for doing so is one of the very important features of these networks where "learning by example" replaces "programming" in solving problems. This feature renders these computational models very appealing in application domains where one has little or incomplete understanding of the problems to be solved, but where training data are available. After training, the neural network can be used to recognize data that is similar to any of the examples shown during the training phase. The neural network can even recognize incomplete or noisy data, an important characteristic that is often used for prediction, diagnosis or control purposes [60].

3.2 Brief History

The earliest work in ANN goes back to the 1940s when neurophysiologist McCulloch and mathematician Pitts [44] introduced the first model of a neuron. In order to describe how neurons in the brain might work, they modeled a simple neuron network using electrical circuits. Their neural network was then used to model logical operators. Following this work, in the late fifties, Rosenblatt [49] introduced the concept of the perceptron, which was capable of learning certain classifications by adjusting connection weights. The early sixties began with high expectations coming off early successes in this theoretical field. Neural networks had built up a lot of hype as the idea of "thinking machines" caught on. However, Minsky [45] demonstrated in 1969 that the perceptron has a lot of limitations and that non-linear classifications, such as exclusive-or (XOR) logic, were impossible. The analysis in Minsky's paper challenged incipient neural theory by establishing criteria for what a particular network could and could not do. The attack was clinical and precise. The effect of this paper was devastating and it led to the decline of the field of neural networks in the next decade [7].

The interest in neural networks was to be renewed though. In 1982, John Hopfield [23] designed a neural network that revived the technology, bringing it out of the dark ages of the 1970s. In the late 1980s, the interest in neural network research increased with new inventions like Self-Organizing Map (SOM), Boltzmann machine, and back-propagation (BP) algorithm. When ANN attracted attention and interest once more, its promises were not artificial brains but the more realistic goal of useful devices. Currently, interest in artificial neural networks is growing rapidly. Professionals from such diverse

fields as engineering, philosophy, physiology, and psychology are intrigued by the potential offered by this technology and are seeking applications within their disciplines.

3.3 Basic definitions and Notations

At the most abstract level, a neural network can be considered a "black box" that is able to map the input space to the output space [3], as shown in Figure 3-1.
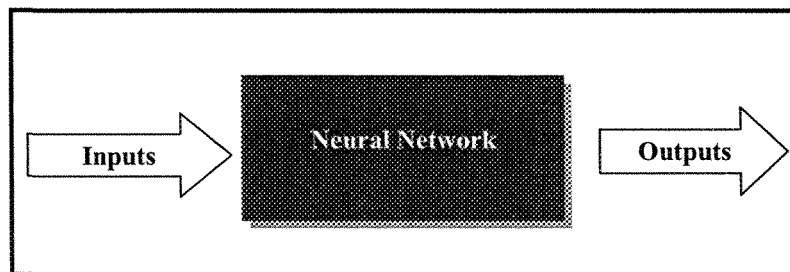
Figure 3-1: General view of Neural Networks as a "black box"

A closer look at the black box reveals that it consists of highly interconnected computing units, also called neurons or processing elements (PEs). In the following sections, the basic elements of a neuron will be described.

3.3.1 The Single Neuron

The neuron is the building block of neural networks. Each neuron is composed of a set of inputs, a body where the processing takes place, and an output. It receives inputs from other neurons in the network, or from the outside world, and calculates an output based on these inputs. Each connection (also called a synapse) between the neurons is given a weight which represents the importance of a specific input. A neural network "learns" by adjusting its weight sets. Figure 3-2 depicts a neuron with n inputs. We can

see that the input signals X_i are transferred into the neuron after being multiplied by synaptic weights W_i. The neuron then computes the sum of the weighted input signals, called net input, and then passes this value through an activation (transfer) function to produce an output value. The neuron also includes an externally applied bias, denoted by b. This bias has the effect of increasing or lowering the net input of the activation function, depending on whether it is positive or negative, respectively [22].
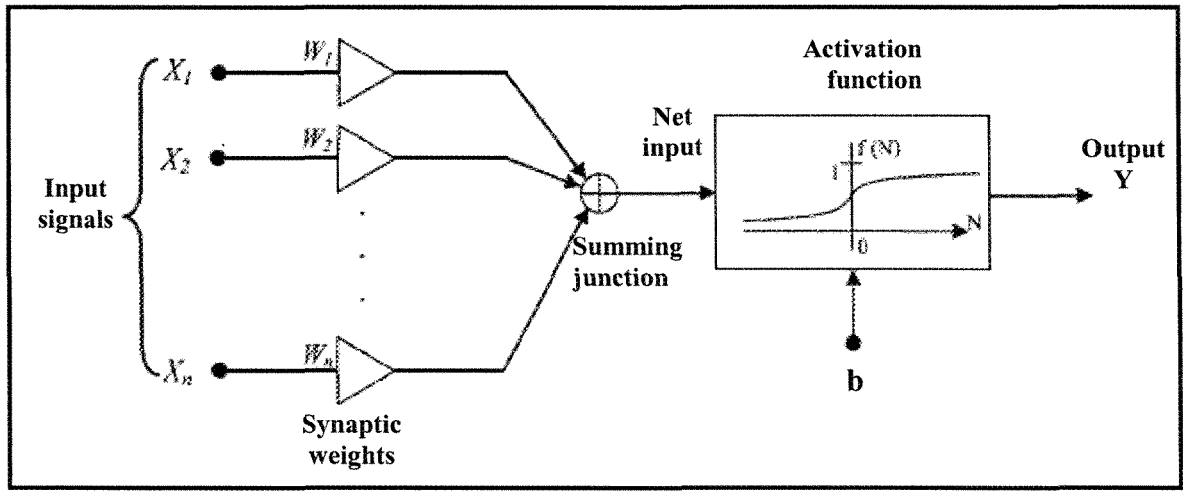
Figure 3-2: A single neuron

In mathematical terms, the following equations give a dense description of the neuron:

$$N = \sum_{i=1}^{n} X_i W_i + b \qquad\qquad \text{3-1}$$

$$y = f(N) \qquad\qquad \text{3-2}$$

where $X_1, X_2, ..., X_n$ are the input signals; $W_1, W_2, ... W_n$ are the synaptic weights of neuron; b is the bias term; N is the net input and $f(.)$ is the activation function.

3.3.2 Activation functions

An activation function is used to transform the activation level (net input) of a neuron into an output signal. The "type" of a particular neuron is determined by its activation function. Activation functions with a bounded range are often called squashing functions [22]. Some of the most commonly used activation functions are:

(i) The threshold function: This function is also known as a binary step function or Heaviside function. It describes the "true or false property" and is often referred to as the McCulloch-Pitts model. For this type of activation function, depicted in Figure 3-3a, we have:

$$f(N) = \begin{cases} 1 & N \geq 0 \\ 0 & N < 0 \end{cases} \qquad 3\text{-}3$$

(ii) The piecewise linear function: This function is similar to the threshold function with an additional linear region. For the piecewise linear function shown in Figure 3-3b, we have:

$$f(N) = \begin{cases} 1 & N \geq \frac{1}{2} \\ v & -\frac{1}{2} < N < \frac{1}{2} \\ 0 & N \leq -\frac{1}{2} \end{cases} \qquad 3\text{-}4$$

(iii) Sigmoid functions: The sigmoid function is the most common form of activation function used in the construction of ANNs. This function is continuous and differentiable and therefore it is mostly used in neural networks trained by back-propagation algorithm (see Haykin[22] for more details). An example of the sigmoid function is the logistic function which is illustrated in Figure 3-3c, and is defined by:

$$f(N) = \frac{1}{1 + e^{-a(N)}}$$

3-5

where a is the slope parameter of the sigmoid function.

As an alternative to logistic function for the applications whose output values range from -1 to +1, we may use the hyperbolic tangent function, also known as bipolar sigmoid function. This function is depicted in Figure 3-3d, and is defined by:

$$f(N) = \tanh(\tfrac{N}{2}) = \frac{1 - e^{-N}}{1 + e^{-N}}$$

3-6

28
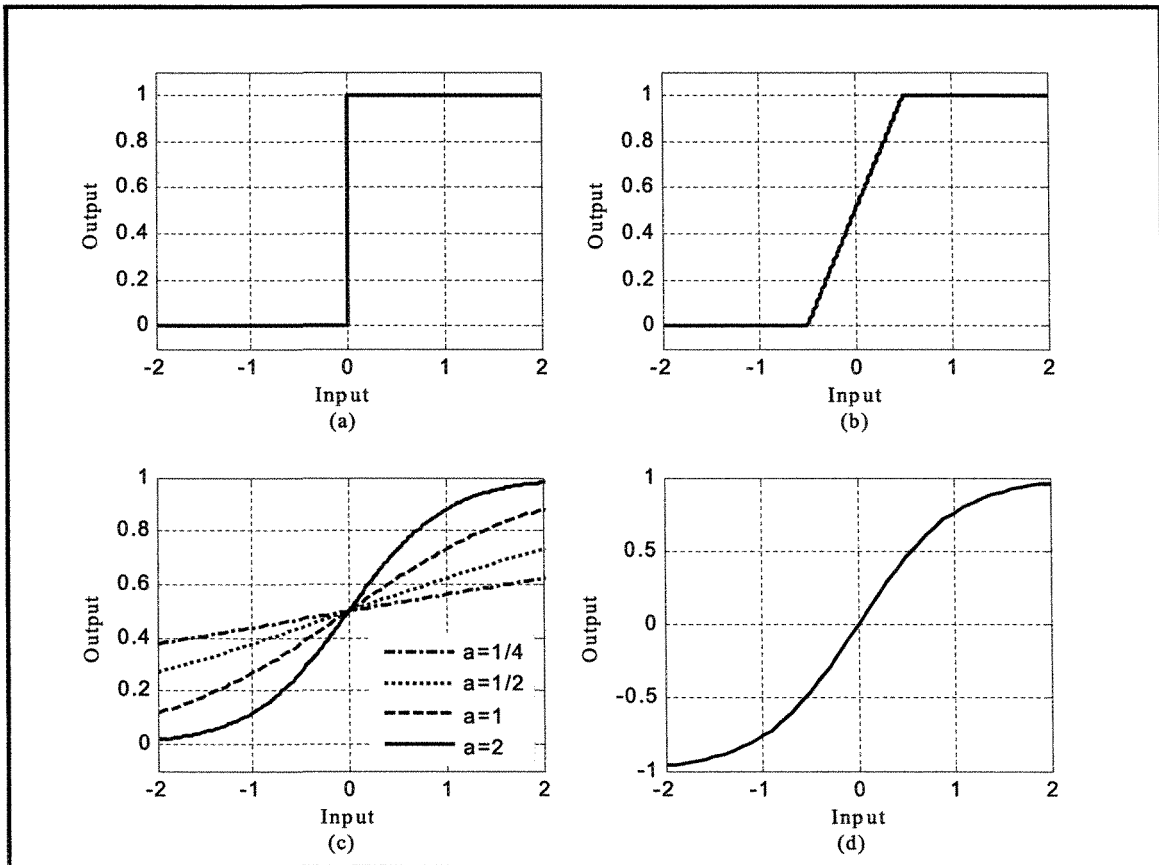
Figure 3-3: Activation functions:

a) Threshold function,
b) Piecewise-Linear function,
c) Logistic function for varying slope parameter a
d) Hyperbolic tangent function

3.4 Network Architecture

The combination of two or more of the neurons shown earlier builds a layer and these layers then connect to one another to construct a NN. The neurons are connected to other neurons by receiving input from and /or providing output to the other units. The neurons which only have output connections are considered "input" neurons, while those which have only input connections are called "output" neurons. In addition, a neural network may have one or more "hidden" neurons which neither receive input nor produce output for the network, but rather assist the network in learning to solve a given problem. The connectivity of neurons within a NN is very critical in its ability to process data. Based on the connectivity pattern between the layers of a neural network, there are different architectures, and the main distinction is between feedforward and recurrent (feedback) networks [1].

3.4.1 Feedforward Networks

In most networks, layers of neurons are connected using a feedforward structure where there are no connections that loop back to neurons that have already propagated their output signal. In the simplest form of feedforward networks, the neurons are organized in one layer: the output layer. In such a network, there is an input layer of source nodes that projects onto an output layer of neurons. This structure is called a single-layer network, referring to the output layer which is the only layer that does the computations [22]. Such a structure is depicted in Figure 3-4, for four input signals and two neurons in the output layer. Each ellipse in the figure represents a neuron as previously shown.
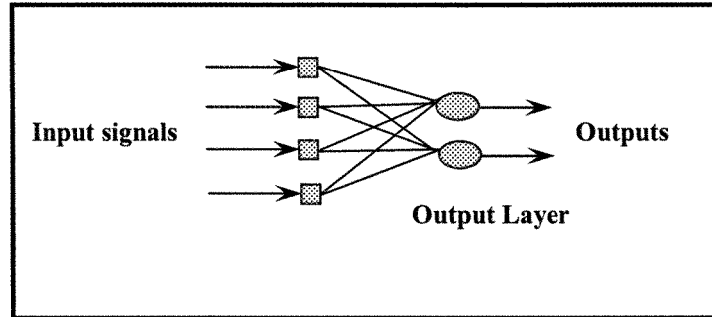
Figure 3-4: An example of single layer feedforward network

A neural network can have one or more hidden layers whose neurons are not connected directly to the output layer as is the case of multilayer neural networks. Extra hidden neurons raise the network's ability to extract higher-order statistics from input data. Multilayer neural networks may be formed by simply cascading a group of single layers. Neurons within the input layer pass their output to the first hidden layer; neurons in this layer then pass their output to the second hidden layer and so on, until eventually the output layer is reached. Figure 3-5 shows a two-layer network with one hidden layer. This network is said to be fully connected in the sense that every node in each layer of the network is connected to every other node in the nearby forward layer. Multi-layer perceptrons (MLPs) are one example of feedforward networks which are the most popular architectures in use today.
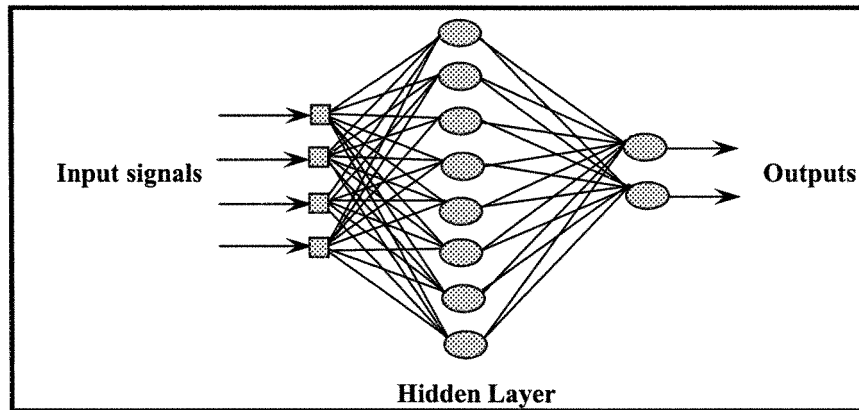
Figure 3-5: An example of multilayer feedforward networks

3.4.2 Recurrent Networks

The other network architectures are recurrent, or feedback, allowing signals to travel to both forward and backward directions by introducing loops in the network. That is, neurons of one layer are able to send their output to previous layers. Recurrent Neural Networks (RNNs) are developed to solve the problems where the solution depends on previous time steps as well as current ones. Specific groups of processing elements called "context units" are added in the input layer that retain the feedback signals from the previous time steps [27]. The outputs of the context neurons can be thought of as external inputs (which are controlled by the network instead of by world events). The first recurrent network was introduced by Jordan in 1986. In this network, there are feedbacks from output units to the context units. That is, the output units are connected to input units but with a time delay, so that the network outputs at time $t-1$ are also the input information at time t. Figure 3-6 shows the structure of the Jordan network.
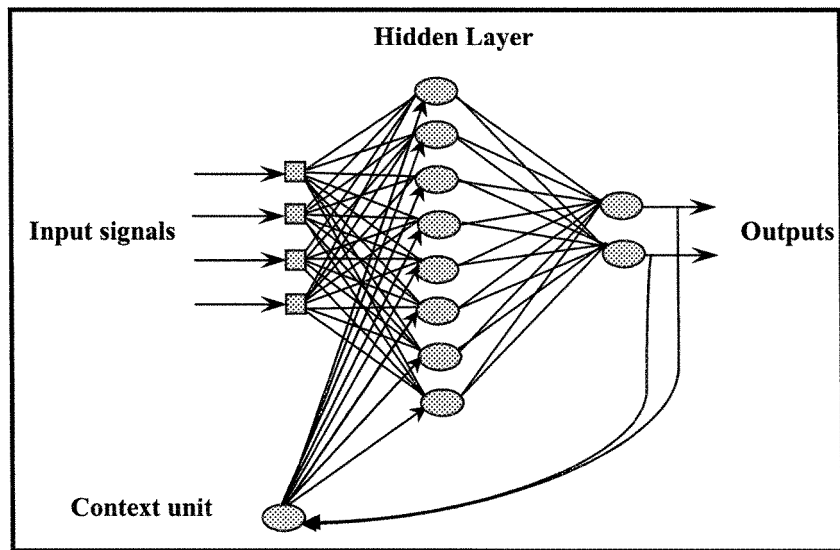
Figure 3-6: Jordan's recurrent network

Another example of RNN is the Elman network [13]. Elman's context layer receives input from the hidden layer as shown in the following figure:
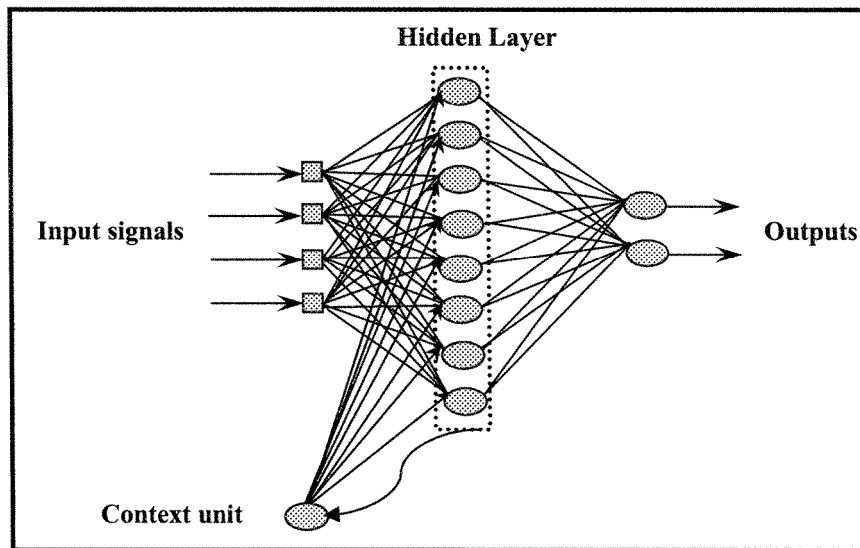
Figure 3-7: Elman's recurrent network

3.5 Learning Process

Once the architecture of an artificial neural network has been determined, it is ready to learn the solution to the problem at hand. The purpose of neural network training is to produce appropriate output patterns for corresponding input patterns. It is achieved by an iterative learning process that updates the neural network weights based on the neural network response to a set of training input patterns. To define the learning process in a more precise manner, we quote the definition offered by Haykin [22]: *"Learning is a process by which the free parameters of a neural network are adapted through a continuing process of stimulation by the environment in which the network is embedded. The type of learning is determined by the manner in which the parameter changes take place. "*

In mathematical terms, if *W (n)* is the value of the weight matrix in time *n*, at this time, an adjustment of ΔW, which is computed as a result of stimulation by the environment, will be applied to the weight matrix yielding the update of the weight matrix for time *n+1* as follows:

$$W(n+1) = W(n) + \Delta W(n)$$

3-1

The way in which the connection weights are updated is known as the learning algorithm. At each training iteration, the learning algorithm determines the new weight for each connection based on past/ or present inputs, outputs, and weights. There are numerous learning algorithms (rules) used for training neural networks. Four basic learning rules are: error-correction learning, Hebbian learning, competitive learning, and Boltzmann learning. (For details of these learning rules, refer to Hykin [22]). The choice

34

of the learning algorithm is dependent on the neural network architecture and the learning paradigm being used.

3.5.1 Learning Paradigms

Broadly speaking, there are two approaches to training neural networks depending on how they relate to their environments: supervised and unsupervised learning.

Supervised Learning: As its name implies, supervised learning is performed under the supervision of an external "teacher". The teacher is considered to have knowledge of the environment that is represented by a set of input-output examples. For each training vector drawn from the environment, the teacher is able to provide the neural network with a desired or target response [22]. By virtue of these targets, the network parameters are adjusted so that the error between the actual response of the network and the desired response is minimized (See Figure 3-8).
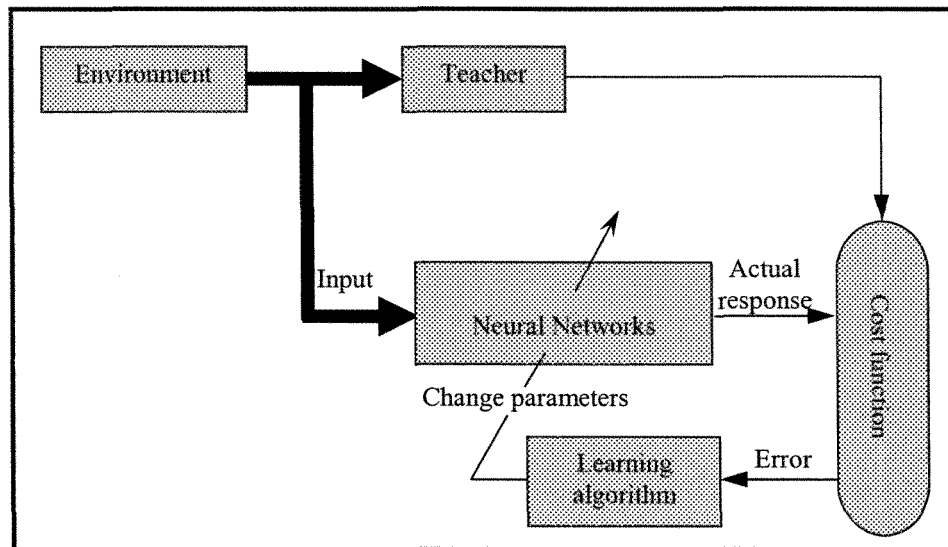
Figure 3-8: Block diagram of supervised learning

35

Unsupervised Learning: This is performed where the network has to process data without any feedback from the environment. Instead, the network's task is to re-represent the inputs in a more efficient way by automatically discovering features, regulations, correlations or categories in the input data. Although unsupervised self-learning networks are closer in function to the brain, researchers have had difficulty implementing them in the solution of real-world problems.
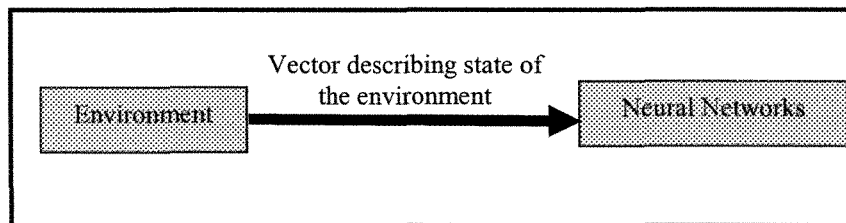
Figure 3-9: Block diagram of unsupervised learning

3.5.2   Learning styles

Aside from these categories of learning process, there are also two learning styles, called Batch training and Incremental training.

Batch training: Batch training of a network proceeds by making weight and bias changes based on an entire set (batch) of input vectors as follows:

1. Initialize the weights
2. Process all the training data
3. Update the weights
4. Unless stop criterion is achieved, go to 2

In the batch or off-line training, once the desired performance for the network is accomplished, the design is "frozen", which means that the neural network operates in a static manner.

Incremental training: Incremental training changes the weights and biases of a network as needed after presentation of each individual input vector, as follows:

1. Initialize the weights
2. Process one training case
3. Update the weights
4. Unless stop criterion is achieved, go to 2

Incremental training is sometimes referred to as "on-line" or "adaptive" training. In this manner, learning is accomplished in real time, with the result that the neural network is dynamic.

3.6 Advantage and disadvantages of neural networks

Neural networks have several advantages. The most important is the ability to learn from data and thus potentially, to generalize, i.e. produce an acceptable output for previously unseen input data (important in prediction tasks). Another valuable quality is the non-linear nature of neural networks; potentially, a vast amount of problems may be solved. Regarding disadvantages, the black-box property first springs to mind. Relating one single outcome of a network to a specific internal decision is very difficult. Another downside of neural networks is overfitting, a problem which sometimes occurs during neural network training. In the case of overfitting, the error on the training set is driven to a very small value, but when new data is presented to the network, the error is large. The network memorizes the training examples, but it cannot learn to generalize to new situations.

3.7 Summary

This chapter is an introduction to the area of neural networks. After a brief survey of chronological progress, the chapter covers all the basic concepts and definitions such as single neuron, transfer function, neural network architectures, learning process and so on. At the end, the advantages and disadvantages of neural networks are discussed.

Chapter 4

Predicting Accreted Ice Type on Exposed Structures

Chapter 4

Predicting accreted ice type on exposed structures

4.1 Introduction

One of the objectives of this study was to investigate the applicability of neural networks in determining types of accreted ice on the structures. In this regard, a preliminary study of the available approaches for determining ice types in the literature was carried out and, based on one of these methods, two training data sets for developing neural network models were created. The first neural network model determines four ice types based on temperature and wind speed variables. A second model was developed with the incorporation of an additional parameter, the droplet size variable. The second model is capable of determining in-cloud ice types.

4.2 Types of ice accretion

The term ice accretion is employed to describe the process of ice growth on a surface exposed to the atmosphere. The ice growth rate on a surface depends on the impact rate of the ice particles, airflow characteristics, and local thermal conditions of the surface [48]. In general, it is recognized that there are four types of ice accretion: hard rime, soft rime, glaze, and wet snow.

Rime is an ice deposit caused by the impact of supercooled droplets which freeze instantly on a surface by losing their latent heat to the surrounding air. This is usually associated with freezing fog. Rime can be formed when the air temperature is well below 0°C (less than -5°C). When the air temperature is below the freezing point, the

supercooled droplets possessing small momentum will freeze instantly on impact, creating air pockets between them. This type of deposit is known as soft rime and has a low density. When the droplets possess greater momentum, or the freezing time is greater, the frozen droplets pack closer together in a dense structure known as hard rime.

Glaze ice will form when the droplet freezing time is sufficiently long for a film of water to cover the accreting surface. Certain water quantities stay unfrozen, and when a second droplet arrives at the same place, it adheres to the previous one. The accretion is accomplished at the water solidification temperature, which is slightly below 0°C at the atmospheric pressure.

Glaze is usually associated with large droplet sizes found in freezing rain incidents. This occurs when there is a layer of below-freezing air near the surface with warmer air aloft. Rain droplets from above fall into the cold layer, and transform to supercooled rain. When these hit the surface, they freeze immediately into a clear glaze ice. Glaze ice is compact, smooth, and usually transparent. It is known by its strong adhesion to surfaces. The density of glaze ice approaches that of bubble-free ice (i.e., 917 kg.m^{-3}) [15]. Rime or glaze icing is commonly referred to as in-cloud icing.

When the liquid water content of the air is high and the air temperature is just above 0° C, the effect of the wind is to produce wet-snow accretion. This form of precipitation can result, for example, in large snow loads on overhead-line conductors. A major property of wet snow is that it may have strong adhesion with the surface of a collector and this property depends on meteorological conditions. The physics of the process of wet snow, however, is not well understood [48].

Usually, the type of accreted ice is determined by assessing the physical properties of the ice including its density, adhesion, color, shape and cohesion. The physical properties of atmospheric ice may vary within rather wide limits. There are also some meteorological parameters affecting ice accretion which can be used to determine the ice type without having to evaluate its physical properties. Typical physical properties and typical values of meteorological parameters are listed in Table 4-1 and Table 4-2 respectively.

Table 4-1: Physical properties of ice[25]

TYPE OF ICE	DENSITY KG/M^3	ADHESION	APPEARANCE		COHESION
			Color	Shape	
Glaze ice	700-900	Strong	Transparent	Cylindrical icicles	Strong
Wet snow	400-700	Medium	White	Cylindrical	Medium to strong
Hard rime	700-900	Strong	Opaque to transparent	Eccentric pennants into wind	Very strong
Soft rime	200-600	Medium	White	Eccentric pennants into wind	Low to medium

Table 4-2: Meteorological parameters controlling ice accretion[25]

TYPE OF ICE	AIR TEMPERATURE	MEAN WIND SPEED	DROPLET SIZE	LIQUID WATER CONTENT	TYPICAL STORM DURATION
Glaze ice	-10<t<0	Any	Large	Medium	Hours
Wet snow	0<t<3	Any	Flakes	Very high	Hours
Hard rime	-10<t<1	10<V	Medium	Medium to high	Days
Soft rime	-20<t<1	V<10	Small	Low	Days

4.3 Developing neural network models to predict ice type

In previous sections, different ways of determining ice type were discussed. As a new approach, we want to develop neural network models to be able to determine ice types, given the meteorological parameters. We want the models to be similar to the following schematic:
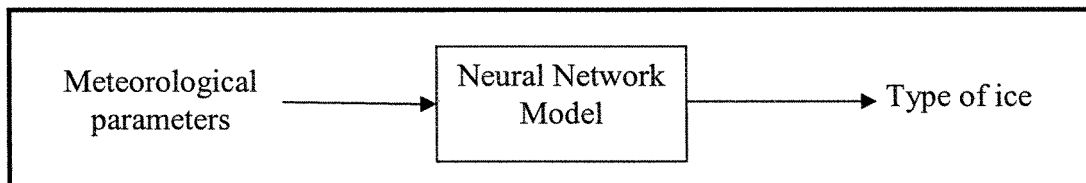
Figure 4-1: The schematic of a neural network model for determining ice types

The first step in developing any neural network model is collecting the data related to the problem. The first thing to do when planning data collection is to decide what data we will need to solve the problem and from where the data will be obtained. Next, we need to make a reasonable estimation of how much data we will need to develop the neural network properly. In the context of our problem, we need a database which attributes the proper ice type to input patterns, which in this case are meteorological parameters. Since, in the available icing databases, there is no information related to ice type, the pertinent literature was used as a source for creating the needed training database. Our strategy was to extract the equations governing the figures offered in the literature and use them as discriminate functions. A discriminate function is used for dividing a set of data points into two different classes [10]. Each data point is substituted in the discriminate function and if the result is equal or greater than zero, the data point is in the right hand of the discriminate or boundary function and if it is less than zero, it is in

the left hand. In summary, each discriminate function divides a given data set into two

sections depending on its sign.

4.3.1   Two-input neural network model

Figure 4-2 recommended by the IEC (International Electrotechnical Commission)

was our first source for creating the necessary training data set. It shows a transient

between soft rime, hard rime, and glaze as a function of wind speed and air temperature.
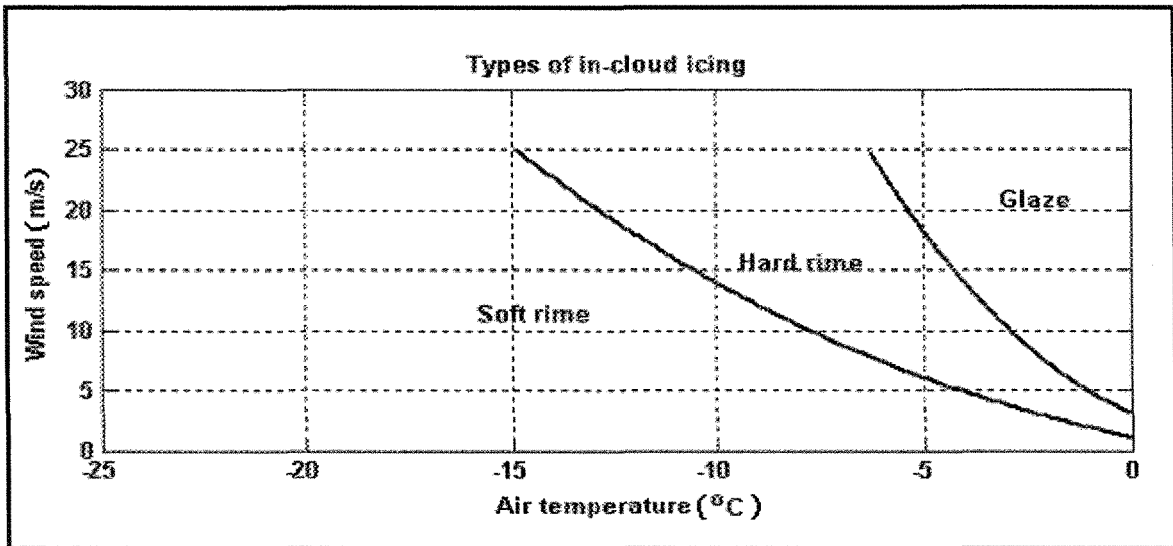
Figure 4-2: Type of accreted in-cloud icing as a function of wind speed and temperature [25]

4.3.1.1   Creating training data set

As the first step for creating the needed data base using the polynomial curve fitting

method, the equations governing the functions of Figure 4-2 were obtained. The first

curve separating glaze ice from hard rime is represented by Equation 4-1 and the second

curve, separating hard rime and soft rime is shown by Equation 4-2.

$$G_1(W,T) = W + 0.001T^3 - 0.045T^2 + 0.746T - 1.085 = 0 \qquad 4\text{-}1$$

$$G_2(W,T) = W + 0.007T^3 - 0.269T^2 + 1.495T - 3.134 = 0 \qquad 4\text{-}2$$

where W is wind speed in m/s and T is temperature in °C.

Using these two discriminate functions, three ice types (glaze, hard rime and soft rime) can be classified. The third discriminate function is obtained from information found in the same reference such as if temperature is greater than zero, regardless of wind speed, the accreted ice type is wet snow.

$$G_3(T) = T \qquad 4\text{-}3$$

In order to create the necessary database, values of temperature and wind speed typical of icing events were considered as input points; then, by using the combination of discriminate functions as shown in Listing 4-1, for each input pair corresponding ice type was determined and saved as the target variable in the data set. Each type of ice was given a specific binary code.

```
If G_3>=0
    ice_type= wet snow coded by [0 0]
elseif G_1>=0
    ice_type=glaze coded by [0 1]
elseif G_1<0 & G_2>=0
    ice_type=hard rime coded by [1 0]
else
    ice_type=soft rime coded by [1 1]
```

Listing 4-1: Pseudo-code for combination of discriminate functions for determining ice types based on temperature and wind speed

Figure 4-3 shows the distribution of the created training data set together with attributed types of ice for related points.
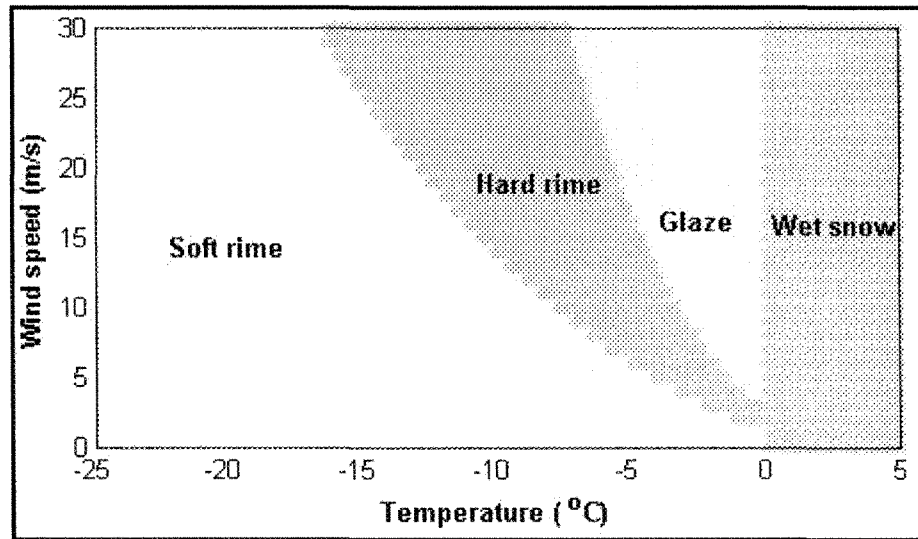
Figure 4-3: Distribution of the points in the created data set for two-input neural network

4.3.1.2   Experimented architectures and performance criteria

The learning task to be dealt with here is a pattern classification problem which the Multi Layer Perceptron (MLP) architecture is the best candidate for solving. The complexity level of the problem is such that only one-hidden layer MLP is sufficient to efficiently reach a solution. The number of input and output neurons is defined by the problem. Figure 4-4 shows the schematic of the chosen architecture. In the input layer, there are two neurons: one for temperature and the other for wind speed. The output layer contains two neurons which represent the binary value of the four possible ice types. The number of neurons in the hidden layer is indicated by j which implies that during the

46

experiments, there were a variable number of neurons in the hidden layer. We began with four neurons in the hidden layer (two times greater than the input neurons) and with each successive test, the number of neurons was increased in order to raise the learning rate of the network. Because of the range of the output, logistic functions were selected as transfer functions for both the hidden and output layers. To perform training, the Levenberg-Marquardt algorithm, one of the fast algorithms of backpropagation training [22], was used.
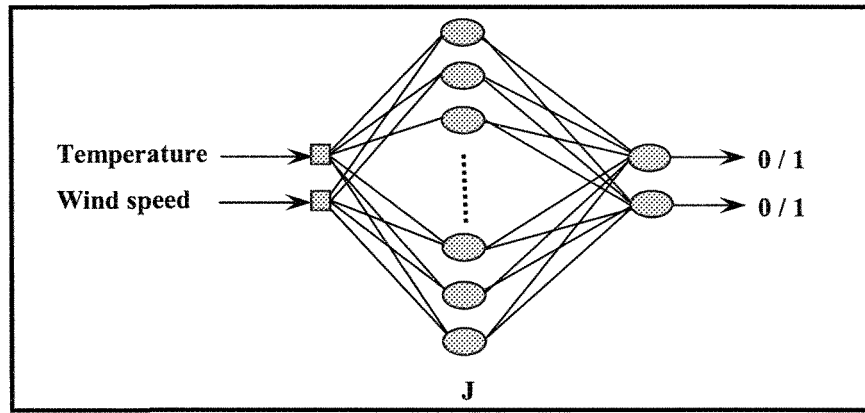
Figure 4-4: Schematic of the experimented architecture for the two-input neural network model for determining accreted ice type

Two criteria have been considered to measure the performance of the model. The first one is the classic Mean Square Error (MSE), which computes the average squared error between the network outputs and the targets. The most efficient model has the least MSE. In mathematical terms, MSE is defined as:

$$MSE = \frac{\sum_{i=1}^{N}(Y_i - \hat{Y}_i)}{N} \qquad \text{4-4}$$

47

where Y_i is the target value , $\hat{Y}_i$ is the output of the network, and N is the number of the training patterns.

The other performance criterion which is the most important criterion for pattern classification problems is the learning rate percentage for each type of ice. Learning rate percentage is defined as the number of the correctly classified input patterns for a specific ice type, divided by the total number of the patterns for that specific ice type, multiplied by 100.

$$Learning\ Rate\ Percentage\ = \frac{Number\ of\ correctly\ classified\ patterns}{Total\ number\ of\ patterns} *100 \qquad 4\text{-}5$$

4.3.1.3 Results of experiments based on MSE and learning rate percentage

In this part, the results of experiments based on MSE are represented. The number of epochs for the tests was set to 10,000 and six different structures were tested. In order to avoid the networks becoming trapped in a local minimum, twenty different tests with a new initiation of weight and bias matrices were carried out for each structure. However, only the best results from twenty repetitions of a specific structure are shown in Figure 4-5. From this figure, it can be concluded that augmenting the number of neurons to ten in the hidden layer decreases the MSE value, thus improving the efficiency of the network. However, the behavior of the network stays almost the same and the error becomes almost zero after a number of neurons larger than 10.

48
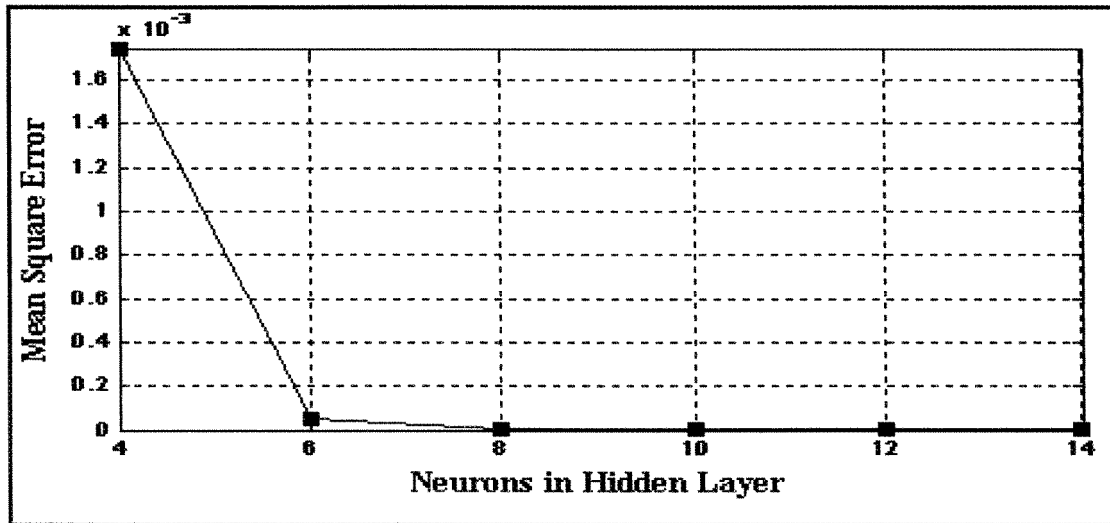
Figure 4-5: Results of experiments for two-input neural network as a function of MSE versus hidden layer's neurons (epochs=10,000)

In order to quantify the classification results for each type of ice, the performance of each structure was tested by running the model with training data and calculating the resulting learning rate percentage. The results are shown in Table 4-3. It is important to mention that in the simulation stage, the output of the network was rounded to the nearest integer. That's why some learning rate percentages reached 100% in spite of the existence of small errors in Figure 4-5. Based on the obtained results, the number of neurons in the hidden layer was set at ten.

Table 4-3: Results of experiments for two-input neural based on learning rate percentage versus hidden layer's neurons

NEURONS IN HIDDEN LAYER	LEARNING RATE (%)			
	Wet snow	Glaze	Hard rime	Soft rime
4	94.21	79.51	83.12	95.11
6	98.14	91.36	94.97	98.46
8	99.08	100	98.31	99.05
10	100	100	100	100
12	100	100	100	100
14	100	100	100	100

4.3.1.4 Validation of the model by icing data of Mont Bélair

In order to validate a neural network model, we apply it to a test data set that was not used during the training process of the network. Here we applied the model for determining the ice type of the icing data which was obtained at the Mont Bélair icing site, 25 km northwest of Quebec City and 9 km north of the Quebec City Airport. Hourly data records were obtained from measurements during 57 consecutive icing events (1739 hours) in the winters of 1998-2000.

First, the ice types of the Mont Bélair data set was determined using the functions proposed in IEC [25] as reference for comparison purposes. Then, using the proposed neural network model, the ice type of this icing data set was determined. The results of the model's performance on this data set have been summarized in Table 4-4, based on the learning rate percentage.

Table 4-4: Learning rate of proposed two-input neural network model for each class of ice type for the Mont Bélair data set

HIDDEN LAYER'S NEURONS	LEARNING RATE (%)			
	Wet snow	Glaze	Hard rime	Soft rime
10	99.95	99.59	100	99.58

It is obvious that for the majority of the data points, ice types were correctly determined by the proposed model. We can conclude that the model is able to perform an ice type determination on new test data with the same accuracy as with the training data set. The visualized results of model's performance on data of Mont Bélair are depicted in Figure 4-6.
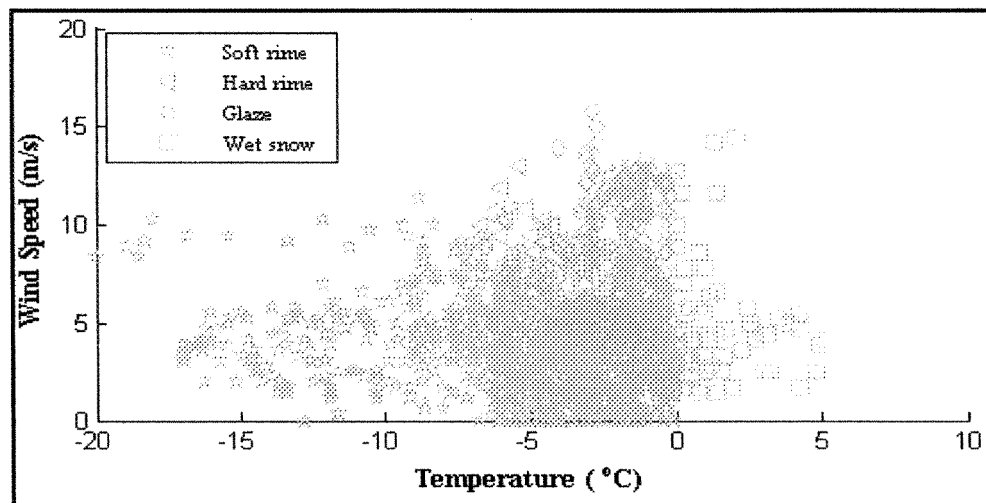
Figure 4-6: Visualized results of proposed two-input neural network model's performance on test data

4.3.2 Three-input neural network model

In spite of the very good results obtained with the developed model, temperature and wind speed parameters are not sufficient to determine a certain ice type. This is why a second model was developed by incorporating an additional parameter: droplet size. The following two figures taken from ref. [11] were our main sources for creating the necessary data set for the second model. The first figure depicted in Figure 4-7 gives the transient between soft rime, hard rime, and glaze as a function of air temperature and wind speed.
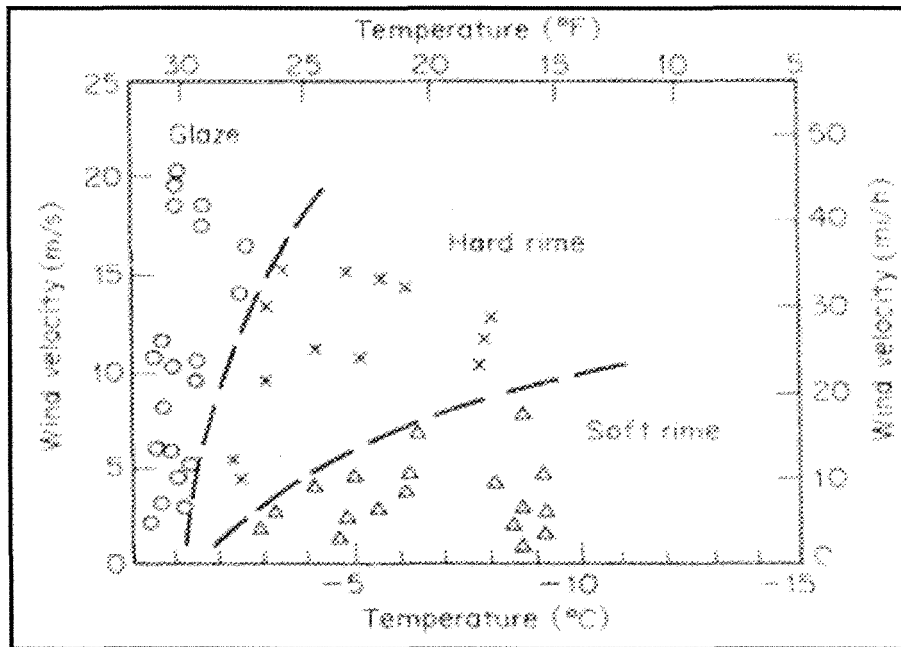
Figure 4-7: Type of accreted icing as a function of wind speed and temperature [11]

The second figure depicted in Figure 4-8 shows the switching between different ice types as a function of air temperature and droplet diameter.
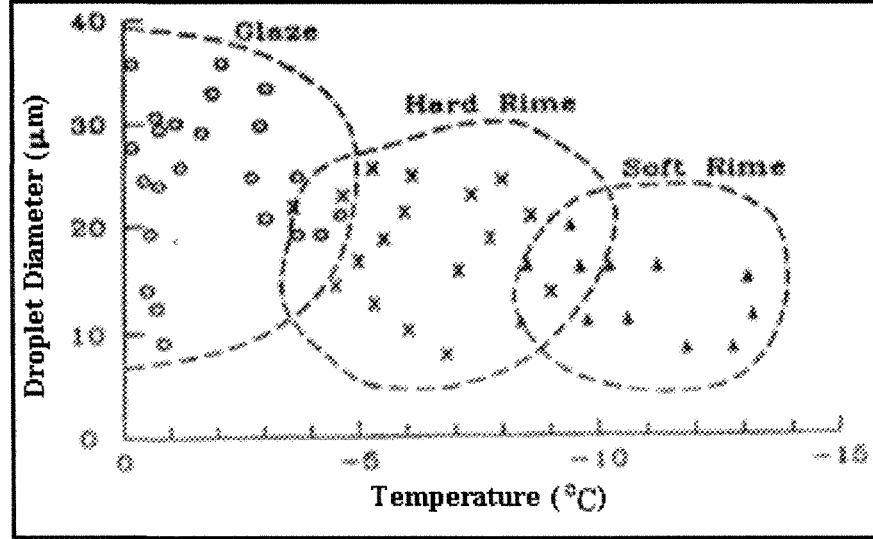
Figure 4-8: Type of accreted ice as a function of droplet diameter and temperature [11]

Similarly, with the development of the two-input model, the equations were estimated from these figures, the first step in creating the training data set. Using the curve-fitting section of Maple software, the following equations were obtained for each of the curves of Figure 4-7. The discriminate function of the first curve separating glaze ice from hard rime is represented by Equation.4-6, whereas the discriminate function of the second curve separating hard rime and soft rime is expressed by Equation 4-7.

$$y_1(W,T) = W + 0.001T^3 - 0.045T^2 + 0.746T - 1.085 = 0 \qquad \text{4-6}$$

$$y_2(W,T) = W + 0.007T^3 - 0.269T^2 + 1.495T - 3.134 = 0 \qquad \text{4-7}$$

where W is wind speed in m/s and T is temperature in $^{\circ}$C.

From Figure 4-8, the simplified equations for three regions were obtained, considering all these regions as ellipses. So, the discriminate functions of the regions related to glaze, hard rime and soft rime, are represented by equations 4-8, 4-9 and 4-10 respectively.

$$y_3(T,D) = 1.616T^2 + 0.155D^2 - 7.193D + 42.621 = 0 \qquad \text{4-8}$$

$$y_4(T,D) = 1.849T^2 + 0.135D^2 + 25.097T - 4.788D + 105.486 = 0 \qquad \text{4-9}$$

$$y_5(T,D) = 1.724T^2 + 0.145D^2 + 38.562T - 4.261D + 232.319 = 0 \qquad \text{4-10}$$

The combination of these discriminate functions, as shown in Listing 4-2, was used to create the target variable corresponding to the ice types in the training data set.

```
If y2>0 & y3<0 & y4>0
    ice_type= glaze coded by [0 0]
elseif y1>0 & y2<0 & y4<0 & y3>0 & y5>0
    ice_type=hard rime coded by [0 1]
elseif y1<0 & y5<0 & y4>0
    ice_type=soft rime coded by [1 0]
else
    ice_type= undecided coded by [1 1]
```

Listing 4-2: Pseudo-code for combination of discriminate functions for determining ice type based on temperature, wind speed and droplet size

As seen from the pseudo-code in Listing 4-2, only three ice types can be determined by the combination of these discriminate functions. This is because it proved impossible to find any information regarding wet snow as a function of temperature, wind speed, and droplet size. Glaze, hard rime, and soft rime are referred to as in-cloud icing in the literature. Therefore, this second model will be used only for predicting in-cloud icing. Figure 4-9 shows the 3D distribution of the created data points. Also, in order to have a better idea of the created data points, Figure 4-10 and Figure 4-11show the projection of these points in 2 dimensions. The white areas in these figures are the regions for which an ice type cannot be determined by the discriminate functions. As shown, the uncertainty region (white area) is much larger than the regions for which an ice type was attributed. However, the available sources in the literature provide only that much information.
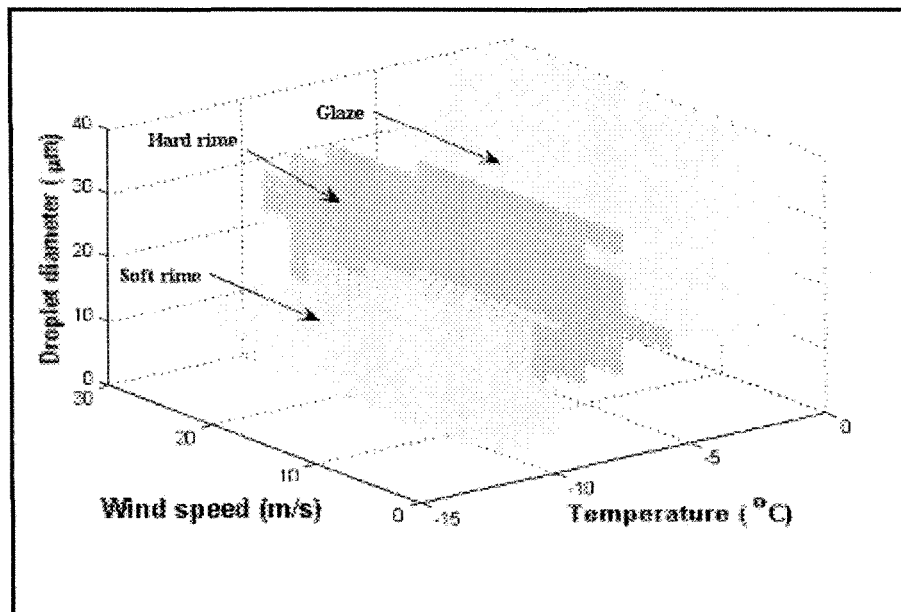
Figure 4-9: Distribution of the points in created data set for the three-input neural network

55
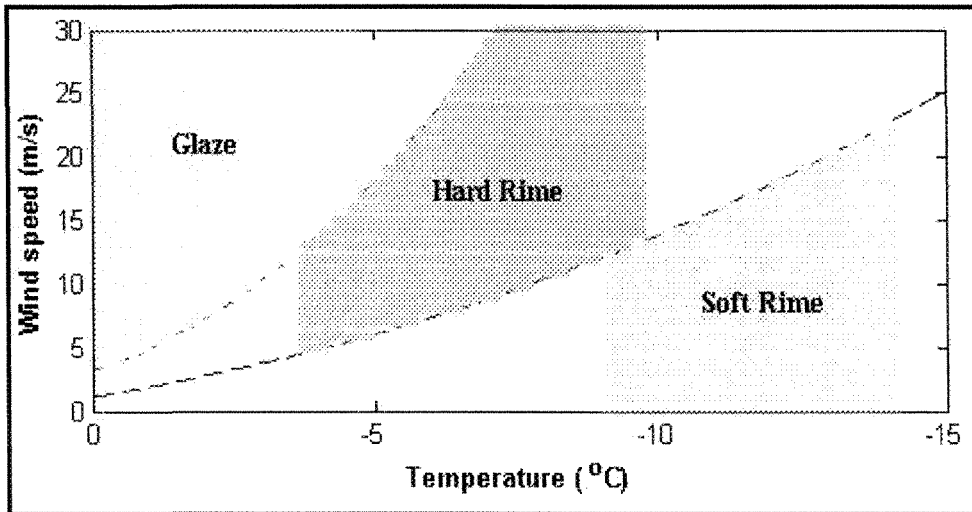
Figure 4-10: The view of created data points for the three-input neural network in 2-dimensions (temperature and wind speed)
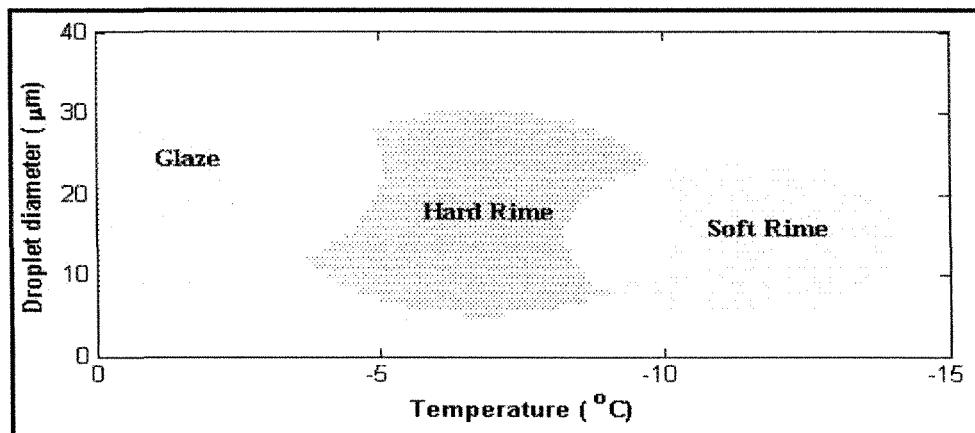
Figure 4-11: The view of created data points for the three-input neural network in 2-dimensions (temperature and droplet diameter)

4.3.3 Experimented Architecture

As was the case for the previous model, a one-hidden-layer MLP with a varying number of neurons in the hidden layer was the experimented architecture. However, there are three input parameters (temperature, wind speed and droplet size) and the number of input neurons is three. In the output layer, there are, once again, two neurons with binary value, their combination representing three ice types (soft rime, hard rime, and glaze). The binary coding of [1 1] means that the neural network is not capable of determining the ice type. The number of hidden layer neurons was varied in order to find the optimum structure for the model. Other characteristics of the network, including transfer function and the learning algorithm, were set as with the two-input model. Figure 4-12 shows the schematic of the chosen architecture for the second model.
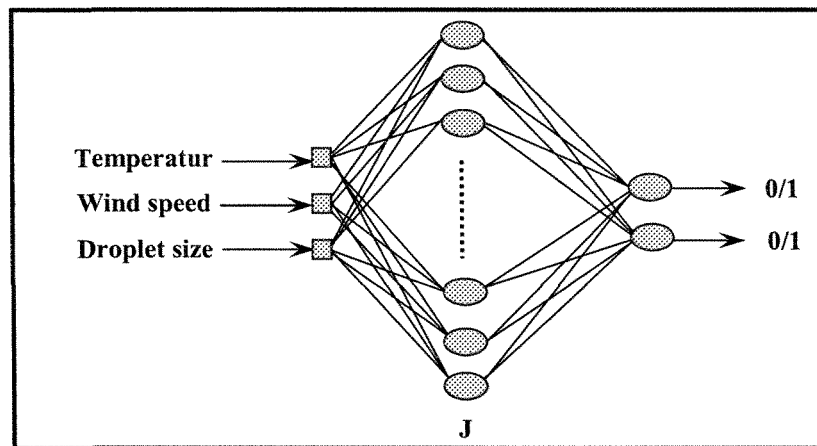
Figure 4-12: Schematic of the experimented architecture for the three-input neural network model for determining accreted ice type

4.3.4   Results of experiments based on MSE and learning rate percentage

Figure 4-13 shows the results of experiments based on MSE for the three-input model. The conditions during the tests were exactly the same as for the previous model. From this figure, it can be concluded that the behavior of the network stays almost the same after a number of neurons larger than 14.
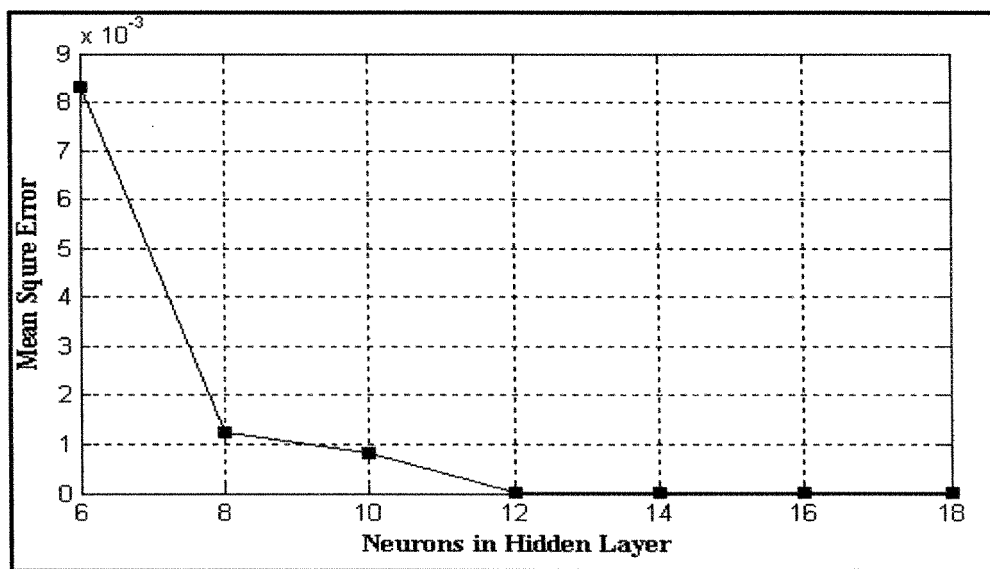
Figure 4-13: Results of experiments for the three-input neural network as a function of MSE versus hidden layer's neurons (epochs=10,000)

The quantified results of classification for each type of ice are shown in Table 4-5. They were obtained by testing the performance of each structure by running it with training data and calculating the resulting learning rate percentages. Based on these results, the number of neurons in the hidden layer was set at 14. Because of the lack of droplet size variables in available icing data bases, the model was not validated, which will be the subject of a future study.

Table 4-5: Results of experiments for the three-input neural network based on the learning rate percentage versus hidden layer's neurons

NEURONS IN HIDDEN LAYER	LEARNING RATE PERCENTAGE			
	Glaze	Hard rime	Soft rime	Uncertain
6	95.37	78.22	85.06	96.24
8	98.56	91.21	84.98	98.47
10	99.09	95.93	95.31	99.05
12	100	99.16	98.49	99.95
14	100	100	100	100
16	100	100	100	100
18	100	100	100	100

4.4 Summary

In this chapter, two models based on neural networks are proposed to predict accreted ice type using meteorological parameters. The data sets for training the models were created using the figures proposed in pertinent literature for switching between different ice types. Because of the pattern classification nature of the problem, one hidden layer MLP was selected as the appropriate architecture to develop these models. The first model is a two-input neural network model which makes use of temperature and wind speed variables as the input parameters for determining four ice types: soft rime, hard rime, glaze, and wet snow. The proposed model was found to have a predictive performance of more than 99% with both training and test data sets.

The second model is a three-input neural network model which utilizes temperature, wind speed and droplet size as input parameters in order to determine in-cloud ice types. The model has a performance of 100% with the training data set. However, because of the lack of a droplet size parameter in the available icing data, it was impossible to validate this model.

It should be noticed that in spite of the good results reported, the accuracy of the models depends on the accuracy of the references used for creating the training data sets. So, such models are valid and reliable as long as the references used for creating training data set are also.

Chapter 5

Predicting Hourly Ice Accumulation Rate on Exposed Structures

Chapter 5

Predicting hourly ice accumulation rate on exposed structures

5.1 Introduction

A large number of high-voltage transmission lines are exposed to atmospheric icing in remote northern regions. Appropriate icing models to estimate transmission-line icing are critical for companies to optimize the design of reliable equipment able to operate in this environment. For electricity companies, ice-load forecasting can help determine the operational impact on their equipment so that serious damage can be avoided. It can also help them find the best possible way to minimize the operational costs of extreme loads. It is apparent from the aforementioned reasons that a reliable load forecast is a must for any kind of operational planning. This chapter covers the development of empirical models for predicting icing load rate on transmission lines based on the neural network technique.

5.2 Description of data source and input icing data

The icing data used for developing the predictive models in this chapter was gathered at the Mont Bélair icing test site in Quebec, which is one of the measuring sites of Hydro-Quebec's SYGIVRE network. A good understanding of this measurement site and the available parameters is the first step of developing the models.

5.2.1 Data Source

Hydro-Quebec is particularly involved in the study of atmospheric icing accumulations on structures, both because of the extension of its power transport network and the meteorological conditions of its environment. In order to improve the monitoring of its power transmission networks, the company has set up a network of measuring stations. The principal measuring instrument used in this network is an autonomous instrument called the Icing Rate Meter (IRM). The function of this network is to collect raw data of atmospheric icing in real time. The raw data collected by IRM at each measuring site is transmitted by micro-wave, satellite, or telephone lines to a central computer that continuously analyses them site by site and converts raw icing data into icing events. This real-time icing event management system is called SYGIVRE [19].

One of the best-equipped measurement stations in the SYGIVRE network is the Mont Bélair icing site, located at Mount Bélair, 25 km northwest of Quebec City and 9 km north of the Quebec City airport. This test site is located at an altitude of 490 m in a corridor formed by the Laurentian Valley. The main winds generally travel northeast (along the axis of the St. Lawrence River) and experience uplift when they pass over Mont Bélair. These characteristics and the presence of two high-voltage transmission lines (315-kV and 735-kV lines) make this site ideal for atmospheric icing observations. It frequently receives all types of atmospheric icing and is therefore a perfect site for ice load measurements. This test site provides measurements of several meteorological parameters: air temperature, wind speed and direction, and precipitation rate. It records mainly wind and ice loads directly on a live 315-kV transmission line. As depicted in Figure 5-1, a load cell (Ontario Hydro's TLSN-10) is installed on the tower which

supports the 315-kV lines. This site is equipped with two heated anemometers as well as an icing rate meter (IRM) and a thermistor, both located on the 315-kV lines at 12 m and 10 m above the ground respectively. About 15 m away from the 315-kV line, a precipitation gauge is installed [39][51][31].
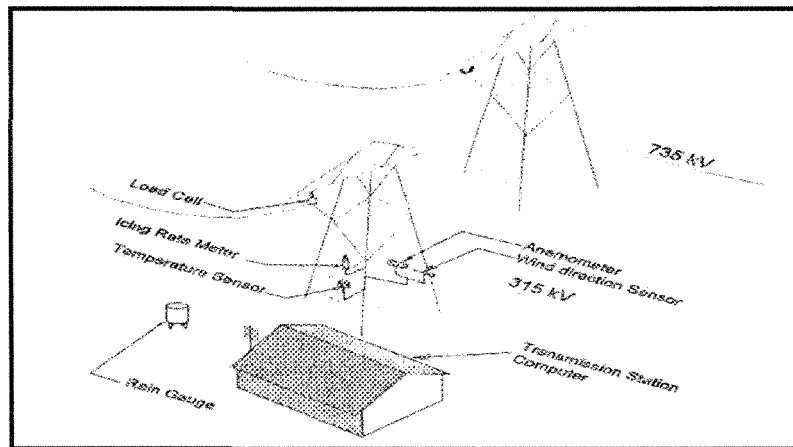
Figure 5-1: Schematic description of the Mont Bélair test site [39]

Developed by Hydro-Quebec for icing detection, IRM consists of a vertical 25.4 mm-long and 6.2 mm diameter cylindrical probe (Figure 5-2). The natural frequency of the probe, e.g. the frequency of vibration without presence of ice on it, is 40 kHz which decreases at a rate of about 2 Hz for each mg of accreted ice [18][43][51]. After an ice accretion of 60-50 mg on the probe, an electronic controller heats and deices the probe, and thus completes a cycle recorded by a cumulative counter. The hourly number of cycles or IRM signals can be used as a warning signal, but also as an indirect measure of the icing rate in the surrounding atmosphere. Each IRM cycle corresponds to 0.009 kg/m in the case of time, and to 0.023 kg/m for glaze [51].
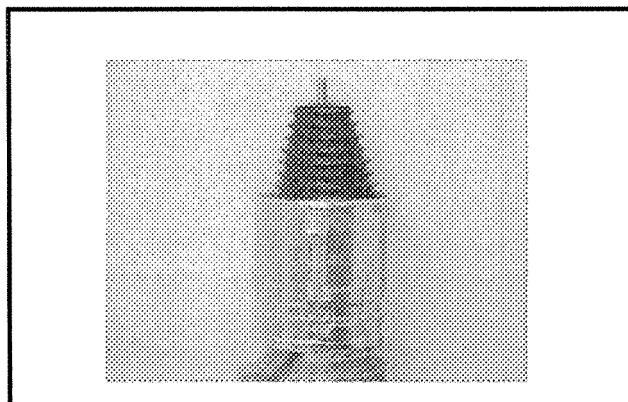
Figure 5-2: Ice Rate Meter

The load cell is incorporated between a suspension insulator string and the cross arm of the instrumented tower. Their readings (in volts) are proportional to the weight of the ice-covered conductor within the weight span L_p (Figure 5-3). Hourly variations of this force are used to estimate the hourly icing rate per unit length of the conductor [18]. The conversion of load cell reading into icing mass in kg can be made using the algorithm proposed in [51].
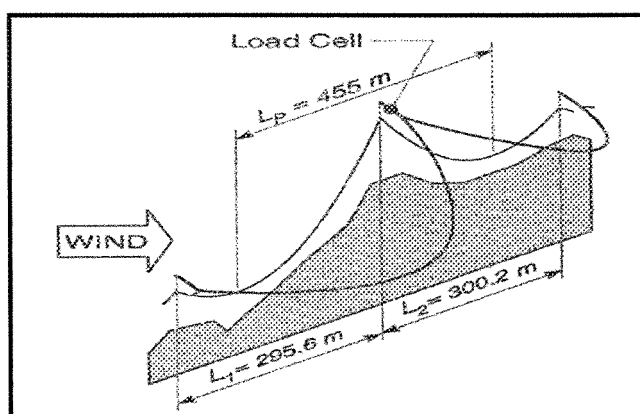
Figure 5-3: Schematic diagram of 315 kV instrumented tower and adjacent spans [18]

5.2.2 Icing Data

Hourly data records, furnished by the Mont Bélair icing test station, were obtained from measurements during 57 consecutive ice events (1739 hours) during the winters of 1998-2000. An icing event as defined in the SYGIVRE database is the total time between a first accumulation of ice on the structure and the complete shedding of ice, which is termed a certified event (CE) [15]. It consists of a combination of three distinct phases, each with a specific duration. The three phases are the accretion phase (ice accretion increases gradually), the persistence phase (the ice stays stable) and the shedding phase (progressive ice loss). Figure 5-4 depicts these three phases for one of the icing events in the database. The icing event depicted in this figure is a typical example although other icing events can have quite different forms.
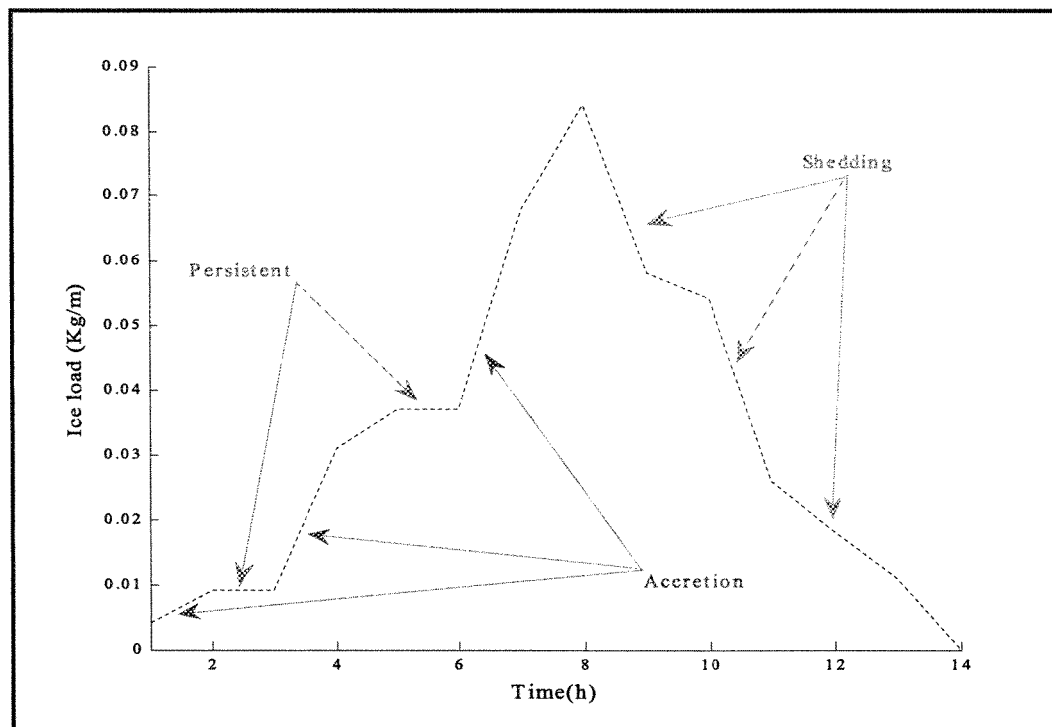
Figure 5-4: The evolution in time of the 21st icing event in the data base

It is important to mention that the data used in this study is not the raw data and it doesn't include the load cell measurements. The raw load cells measurements have been converted to the direct icing rate in (kg/m) by [51]. Table 5-1 shows a part of this data.

Table 5-1: Part of available icing data

Hour.No	Evt.No	Evt.Type	Acc.Rate	Cum.Acc	Temp	MeanSpeed	WindDirec	IRM signal	PrecRate
1	1	2	0.022	0.022	-1.4	23	83	1	2
2	1	2	0.027	0.049	-1.1	26	84	2	5
3	1	2	0.036	0.085	-0.6	25	83	4	5
4	1	2	0.018	0.103	-0.5	23	84	4	3
5	1	2	0	0.103	-0.4	21	89	1	1
6	1	2	-0.034	0.069	-0.3	12	74	0	2
7	1	2	-0.035	0.034	-0.4	10	77	0	6
8	1	2	-0.034	0	-0.1	5	77	0	1
9	2	1	0.032	0.032	-0.9	16	268	2	0
10	2	1	0.001	0.033	-0.6	16	306	2	0
11	2	1	-0.002	0.031	-1.2	19	327	0	0
12	2	1	0	0.031	-1.2	16	295	0	0
13	2	1	-0.002	0.029	-1.7	20	316	0	0
14	2	1	-0.003	0.026	-2.8	26	295	0	0
15	2	1	-0.007	0.019	-4.6	27	302	0	0
16	2	1	-0.011	0.008	-6.1	24	292	0	0
17	2	1	0	0.008	-8.8	26	286	0	0
18	2	1	-0.005	0.003	-10.8	24	286	0	0
19	2	1	-0.003	0	-12.1	25	297	0	0
20	3	1	0.006	0.006	-3.8	19	74	1	0
21	3	1	0.008	0.014	-4	15	72	0	0
22	3	1	0	0.014	-4.1	9	46	0	0
23	3	2	0	0.014	-4	2	89	0	1
24	3	2	-0.001	0.013	-4.3	1	120	0	2
25	3	2	0.002	0.015	-3.8	0	201	0	3
26	3	2	0.008	0.023	-3.9	0	269	0	2
27	3	2	-0.001	0.022	-4	0	254	0	1
28	3	2	-0.002	0.02	-4.7	8	220	0	2
29	3	1	-0.001	0.019	-5.1	15	234	0	0

Mont Bélair

Important parameters beginning from the third column of Table 5-1 are as follows:

- ✓ Type of icing event
- ✓ Hourly icing rate (kg/m/h)
- ✓ Cumulative icing rate (kg/m)
- ✓ Ambient temperature (°C)
- ✓ Mean wind speed (km/h)
- ✓ Wind direction (degrees)
- ✓ Hourly number of IRM signals
- ✓ Precipitation rate (mm/h)

5.2.3 Graphical analysis of data

The aim of this preliminary analysis is to avoid feeding the neural networks with auto-correlated variables. At best, the use of correlated variables overbalances a particular component of the data, and in the worst case, makes the model unstable and provides unreliable results [9]. In order to reveal the existence of correlation between two variables, the scatter plot is used. When plotted, the closer the data points come to making a straight line, the higher the correlation between the two variables or the stronger the relationship. The scatter plot matrix depicted in Figure 5-5 shows that there is no correlation between the temperature, mean wind speed, precipitation rate, wind direction, and number of IRM signals. So, all five variables were used as input parameters to the neural networks.
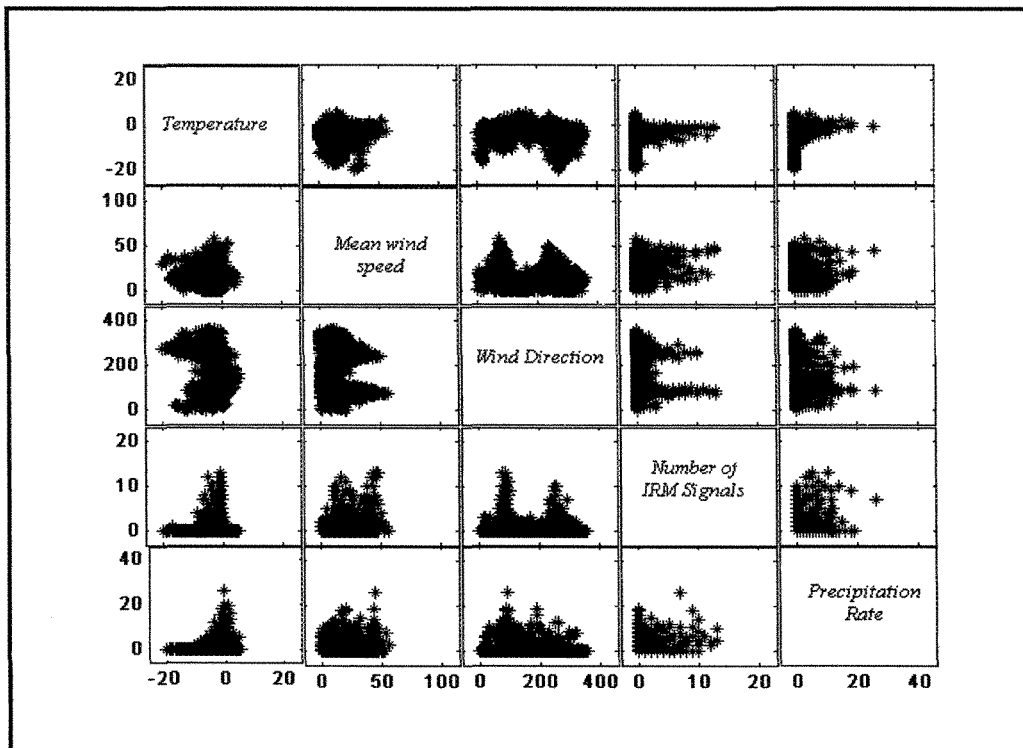

Figure 5-5: Scatter plot matrix of icing data
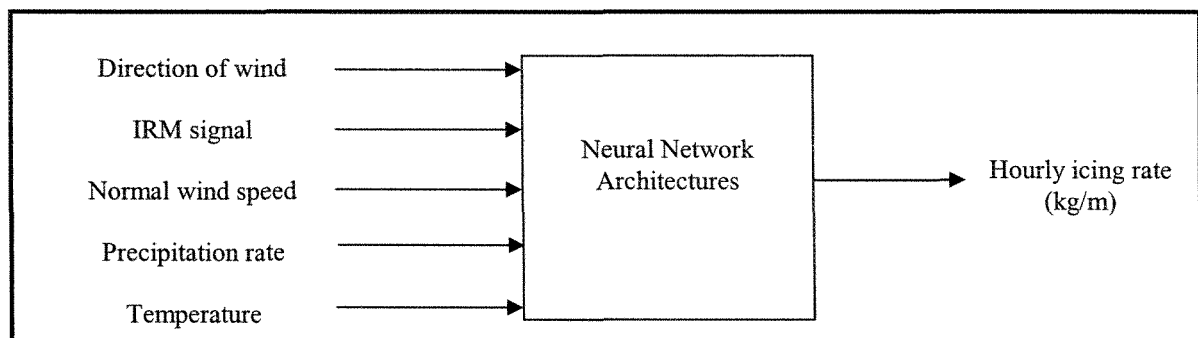
5.2.4 Data preparation and pre-processing

Since in this study our objective was to investigate the utility of data filtering in the efficiency of the neural network model, three data sets were extracted from the main data, considering different filters. The first extracted data set includes all the available data and it will be called the "complete event" data set. The second one was extracted considering only the accretion phase of the icing events and will be called the "accretion phase" data set. Finally, the third data set, called the "precipitation events" data set, was created considering only the events that were marked as precipitation icing in the main data set. Each of these data sets was then partitioned into training and validation sets. Because of the limited number of data points available in the main data set, we had to consider 80% of the points as training data sets and 20% as validation. At the last stage, all the data sets were normalized so that they had zero mean and unity standard deviation.

5.3 Experimented architectures and performance criterion

Though theoretically there is a network that can simulate a problem to any accuracy, there is no easy way to find it. To choose a network architecture and to define its exact structure, such as how many hidden layers should be used, how many neurons should there be within a hidden layer for a certain problem, is always a painful job and it involves much trial and error. The approach taken in the context of this work was to use the most homogeneous data set, which is the "accretion phase" data, together with "nowcasting" learning task in the initial experiments. "Nowcasting" means that the neural networks are not trained for prediction. Rather, their task is learning to represent the nonlinear mapping between the input parameters and the ice accretion rate. By doing the

initial experiments in the "nowcasting" mode, the configurations of each of the tested architectures that had the best performance in mapping between input parameters and ice load rate were selected as candidates for developing predictive models. These initial experiments were the most time-consuming part of this study. Nearly two hundred different configurations were tested and for each configuration two learning styles, batch and incremental learning were examined and compared.

The experimented architectures during this segment can be divided into two global categories: feedforward networks, which can also be considered static networks, including one-hidden layer MLP and two-hidden layer MLP, and also recurrent networks considered dynamic networks, including Jordan and Elman. For all networks, the number of input neurons and the number of output neurons was fixed to five and one, respectively. The number of neurons in the hidden layer was the varying parameter for finding the optimum structure. The following figure shows the schematic of the model.

Direction of wind →
IRM signal →
Normal wind speed → Neural Network Architectures → Hourly icing rate (kg/m)
Precipitation rate →
Temperature →

Figure 5-6: Global schematic of the experimented architectures

For the transfer function of the neural networks, tangent hyperbolic was used for all the hidden layers with all the architectures. Initially, for the output layer, a linear function was tested but the results showed that it yields to the odd values which are far from the range of the output variables. To avoid this type of problem, the tangent hyperbolic function was used for the output neurons as well.

In order to measure and compare the performance of the different structures, we need a performance criterion. The performance function widely used in neural networks is the MSE function. However, this function does not take into account dispersal of the data. The criterion selected for measuring the performance of the models in this part is Normalized Mean Square Error (NMSE). It is defined as the division of MSE to the variance of data. The reason for using this criterion instead of the classic MSE is that it takes into consideration the dispersal of data sets and is a more reasonable criterion to be used in working with different data sets. . In mathematical terms, NMSE is defined as:

$$NMSE = \frac{1}{\sigma^2 N} \sum_{i=1}^{N} (I_i - \hat{I}_i)^2 \qquad 5\text{-}1$$

where I_i is the real value of the ith point in the series of data of length N, $\hat{I}_i$ is the predicted value and σ is the standard deviation of the real series of data during the prediction interval. The lower this value, the better a model is.

5.4   Results of initial experiments based on NMSE

Here, the results of initial experiments with different configurations for each of the four architectures are represented. These include the results of both batch and incremental learning styles with the "accretion phase" data set. In order to avoid the networks becoming trapped in a local minimum, twenty different tests with a new initiation of weight and bias matrices were carried out for each configuration but the presented results are the best from the twenty tests.
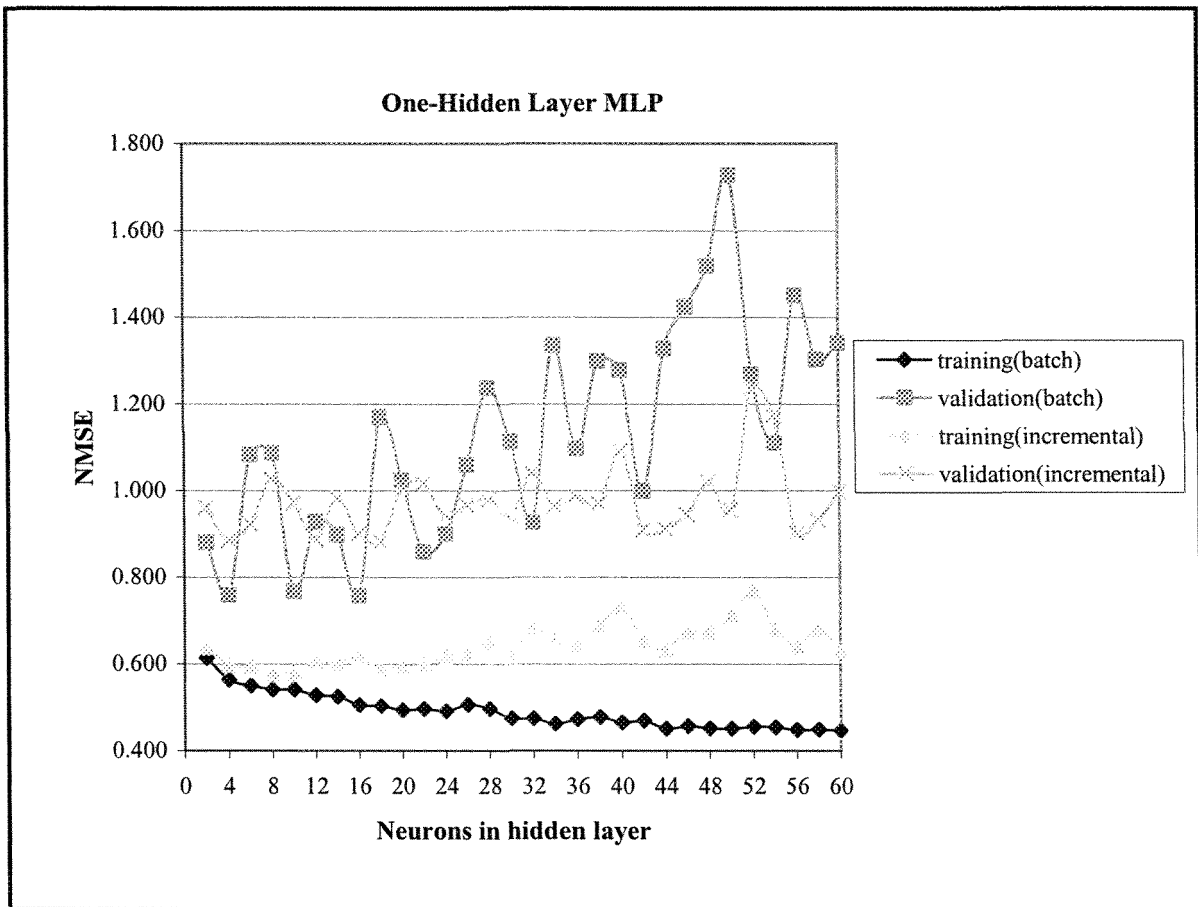
Figure 5-7: Performances of experimented structures based on NMSE for one-hidden layer MLP
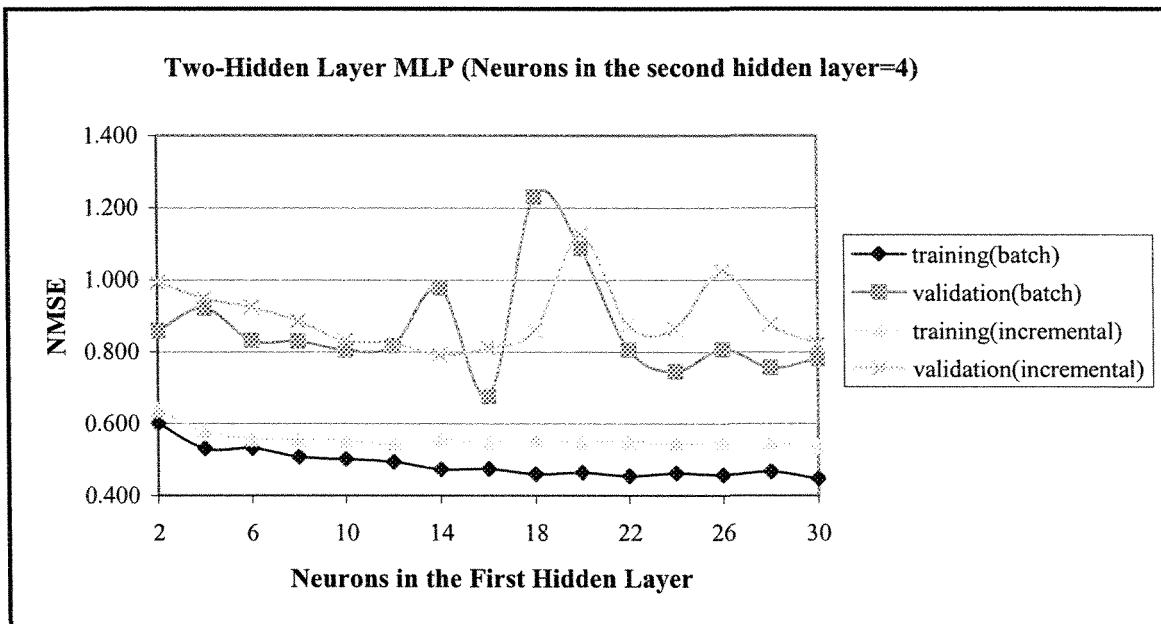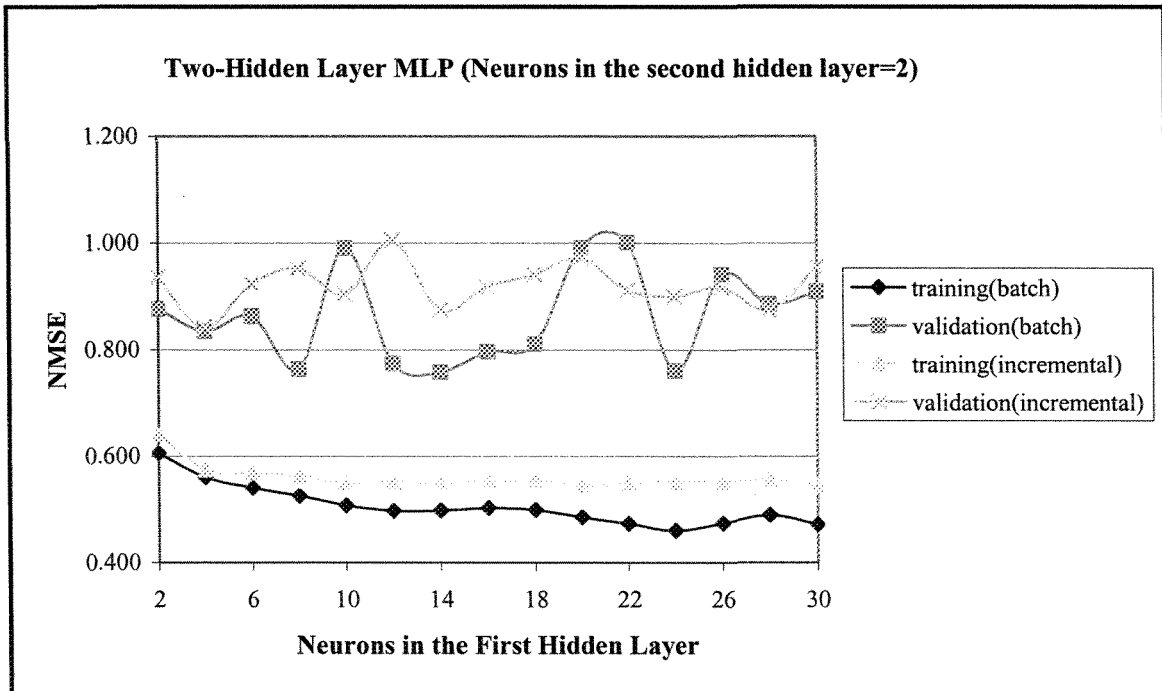
Figure 5-8: Performances of experimented structures based on NMSE for two-hidden layer MLP (Neurons in second hidden layer=2 (top), Neurons in second hidden layer=4 (bottom))
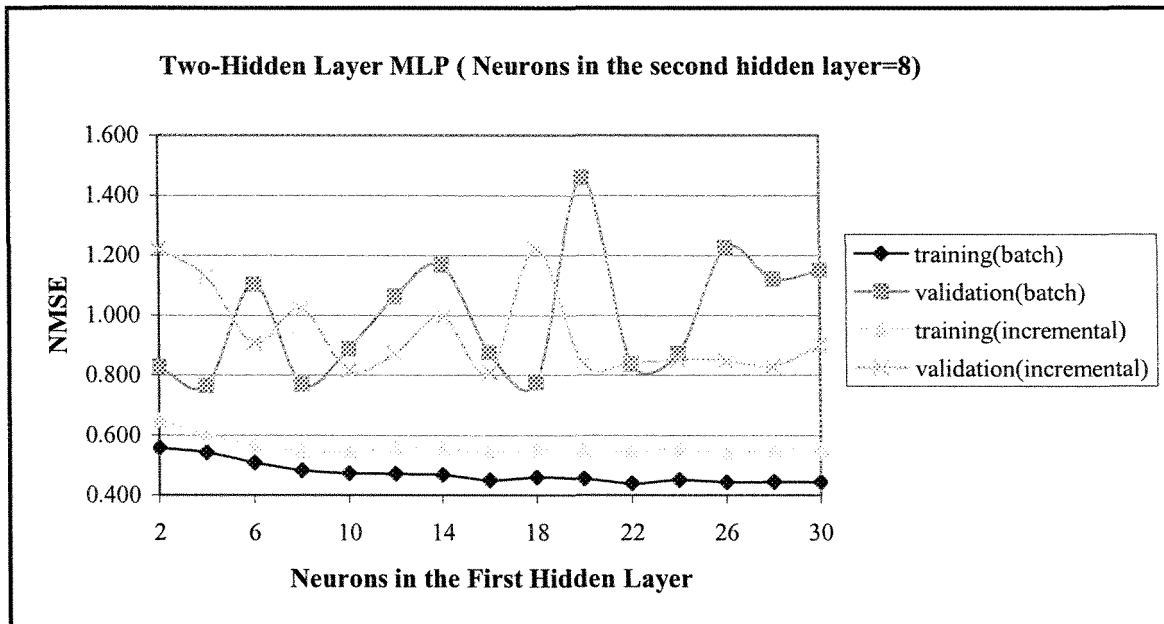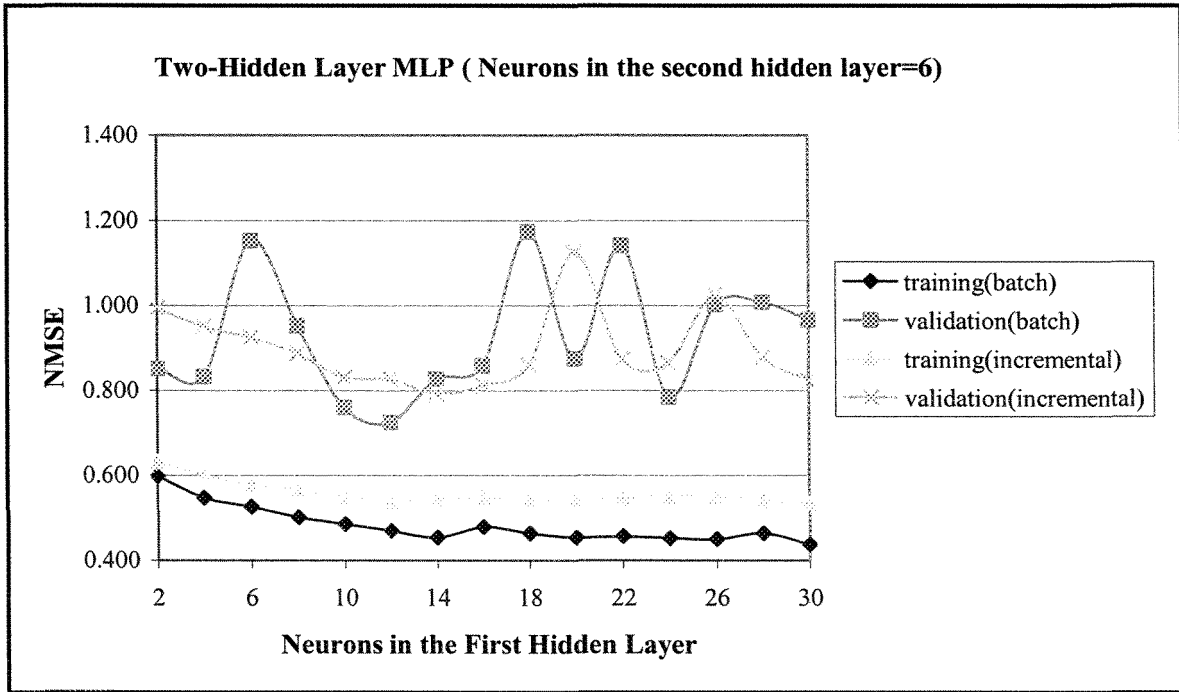
Figure 5-9: Performances of experimented structures based on NMSE for two-hidden layer MLP (Neurons in second hidden layer=6 (top), Neurons in second hidden layer=8 (bottom))

Figure 5-10: Performances of experimented structures based on NMSE for Elman
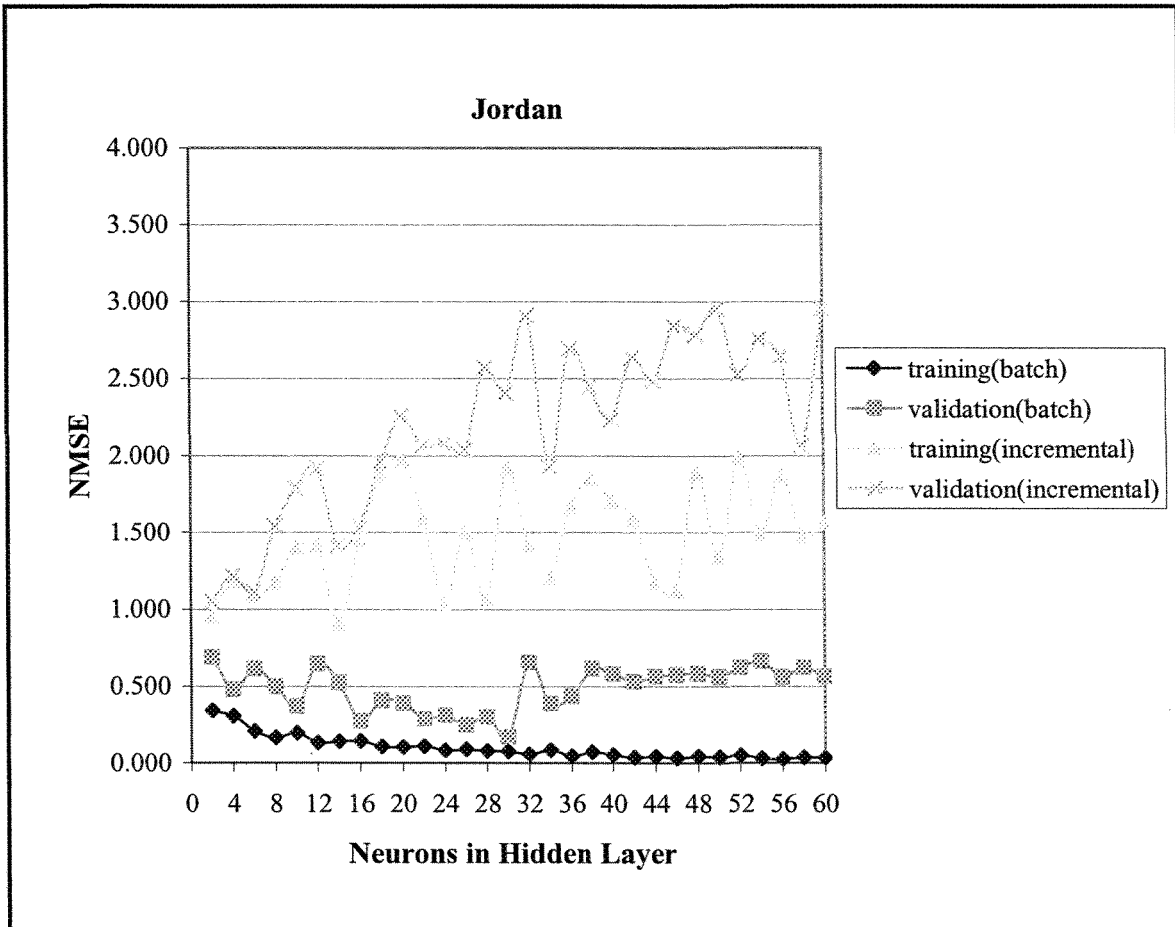
Figure 5-11: Performances of experimented structures based on NMSE for Jordan

Two important facts can be observed in these results. First, although increasing the number of the hidden layer's neurons decreases the NMSE for training sets, in the validation set, there is no such tendency and the results are chaotic in nature. Also, it is obvious that the batch learning style has better results with all architectures. The configurations giving the minimum NMSE with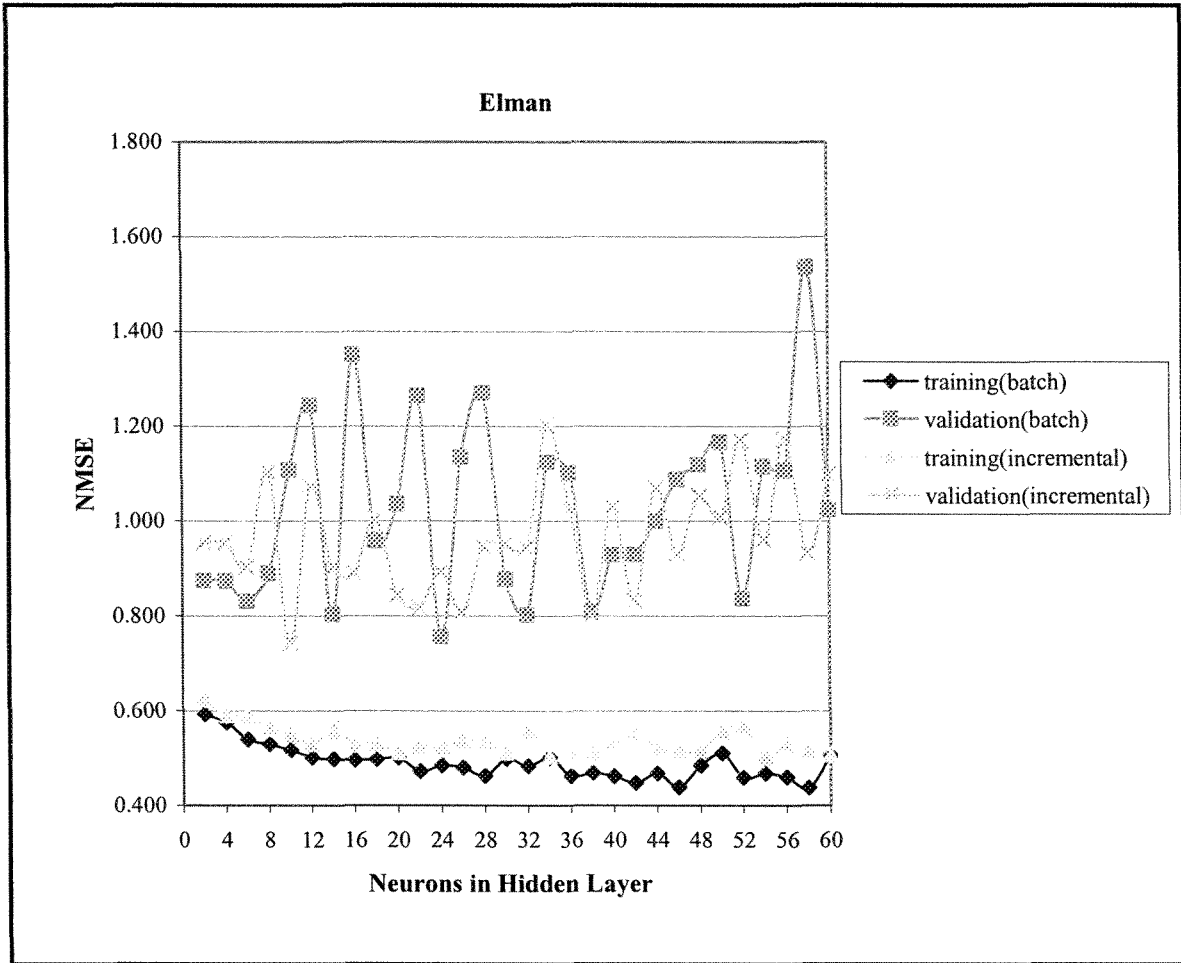 validation sets include one-hidden layer MLP with 16 neurons in the hidden layer, two-hidden layer MLP with 16 neurons in the first hidden layer and 4 neurons in the second hidden layer, Elman with 24 neurons in the hidden layer and finally Jordan with 30 neurons in the hidden layer. These configurations were selected as the candidates for developing predictive models. In order to make the comparisons between the four architectures, the average values of NMSE for each of them are plotted in Figure 5-12.

Figure 5-12: Comparison of the performance of the four experimented architectures

Figure 5-12 leads to the following conclusions:

1. The learning style that produces the best results for all of the architectures is the batch learning style. Therfore, it was concluded that batch lear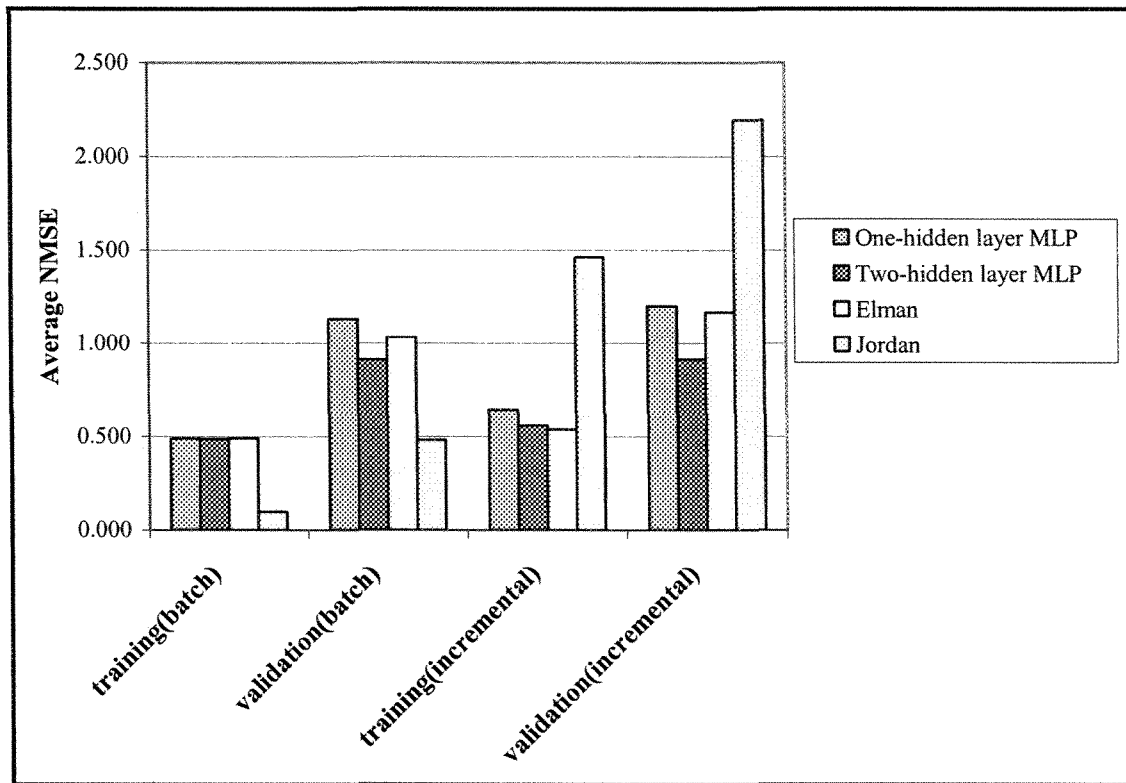ning style is the best style for our problem. The difference between two learning styles is more obvious for the Jordan network.

2. For FFNN, it can be seen that adding a second hidden layer distinctly increases the performance of the network and a two-hidden layer MLP gives better results both with the training data set and the test data set.

3. For RNN, Jordan's network results, in the case of batch learning style, are better than Elman's network results. Although it is difficult to justify these results, we can suppose that the nature of the data is such that the previous value of ice accretion has more predictive power than the previous values of meteorological parameters.

4. In the case of comparison between the four architectures in the batch learning style, Jordan is the architecture that gives the best results for both of the training and test data sets.

5.5 "Nowcasting" curves for the best configurations of initial experiments

To have a better idea of the performance of the four architectures, the performances of the four optimum structures were tested by simulating them with test data sets. The "nowcasting" curves are depicted in the following figures. It is important to remember that the best configurations (optimum structure) have been selected using the structures of neural networks that give the least NMSE with the test data set. These include the one-

hidden layer MLP with 16 neurons in the hidden layer, the two-hidden layer MLP with 16 neurons in the first hidden layer and 4 neurons in the second hidden layer, Elman with 24 neurons in the hidden layer, and finally Jordan, with 30 neurons in the hidden layer.
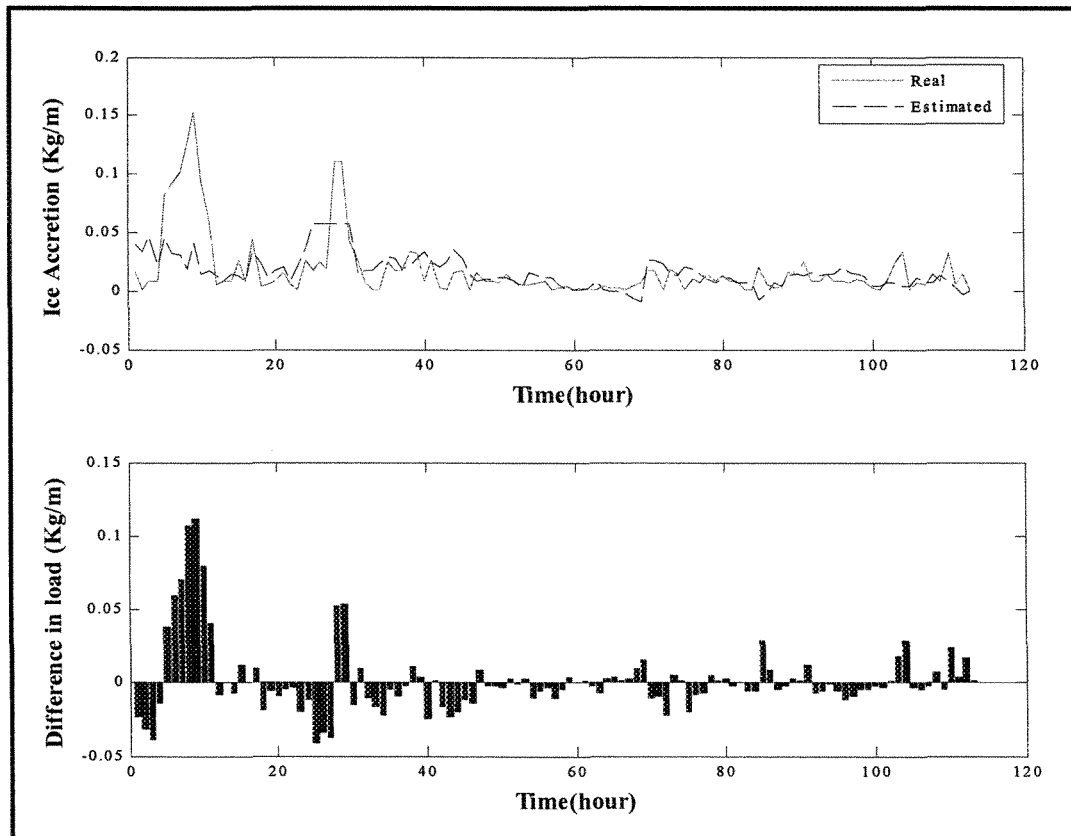
Figure 5-13: "Nowcasting" results of the optimum structure of one-hidden layer MLP with test data set (top), Error bar (bottom)
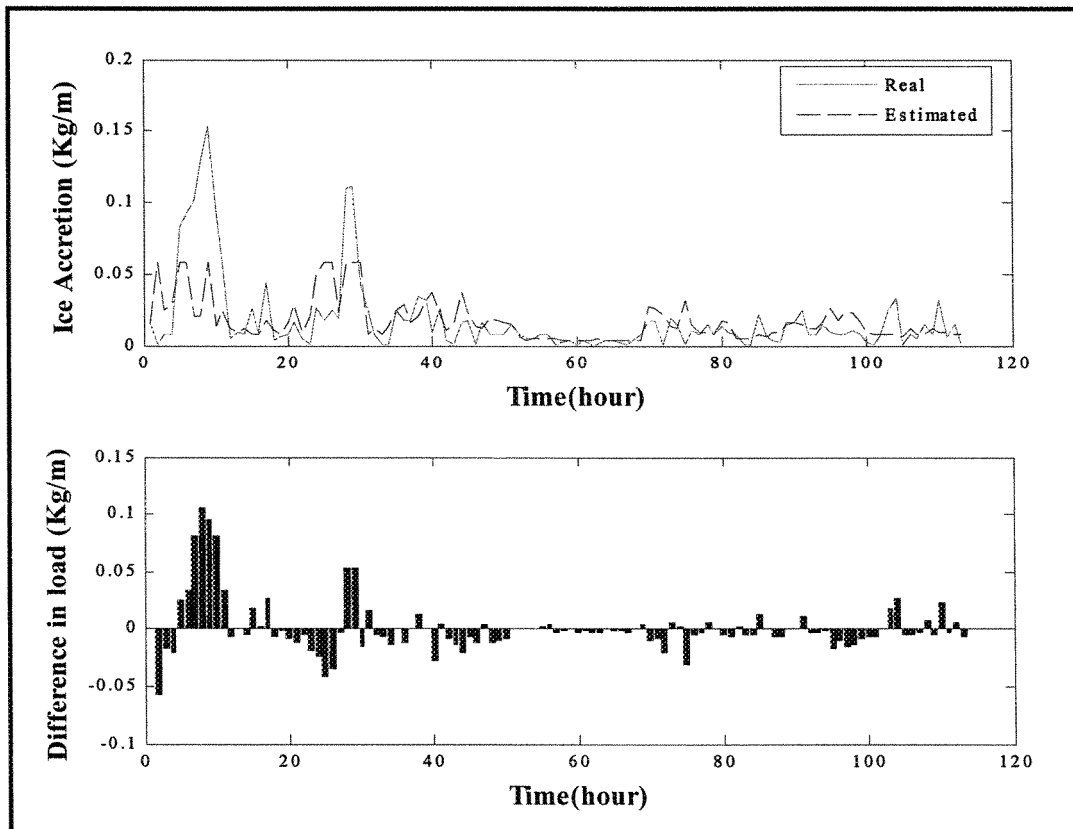
Figure 5-14: "Nowcasting" results of the optimum structure of two-hidden layer MLP with test data set (top), Error bar (bottom)
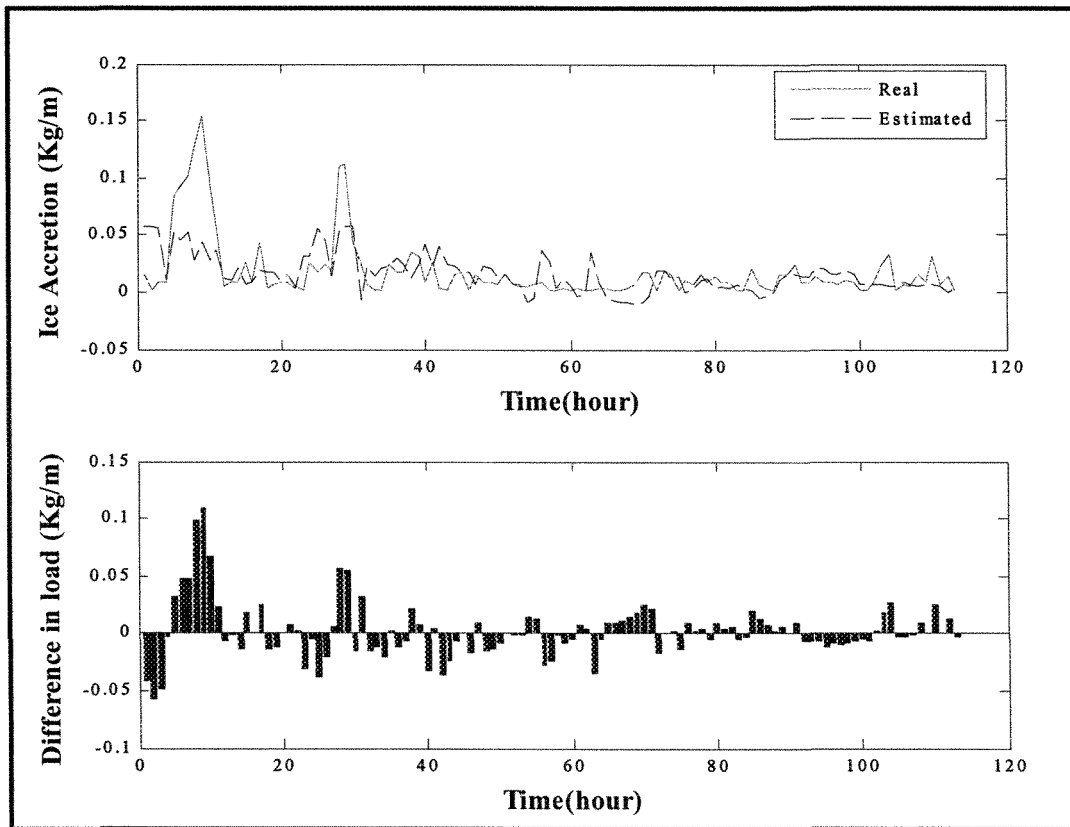
Figure 5-15: "Nowcasting" results of the optimum structure of Elman with test data set (top), Error bar (bottom)
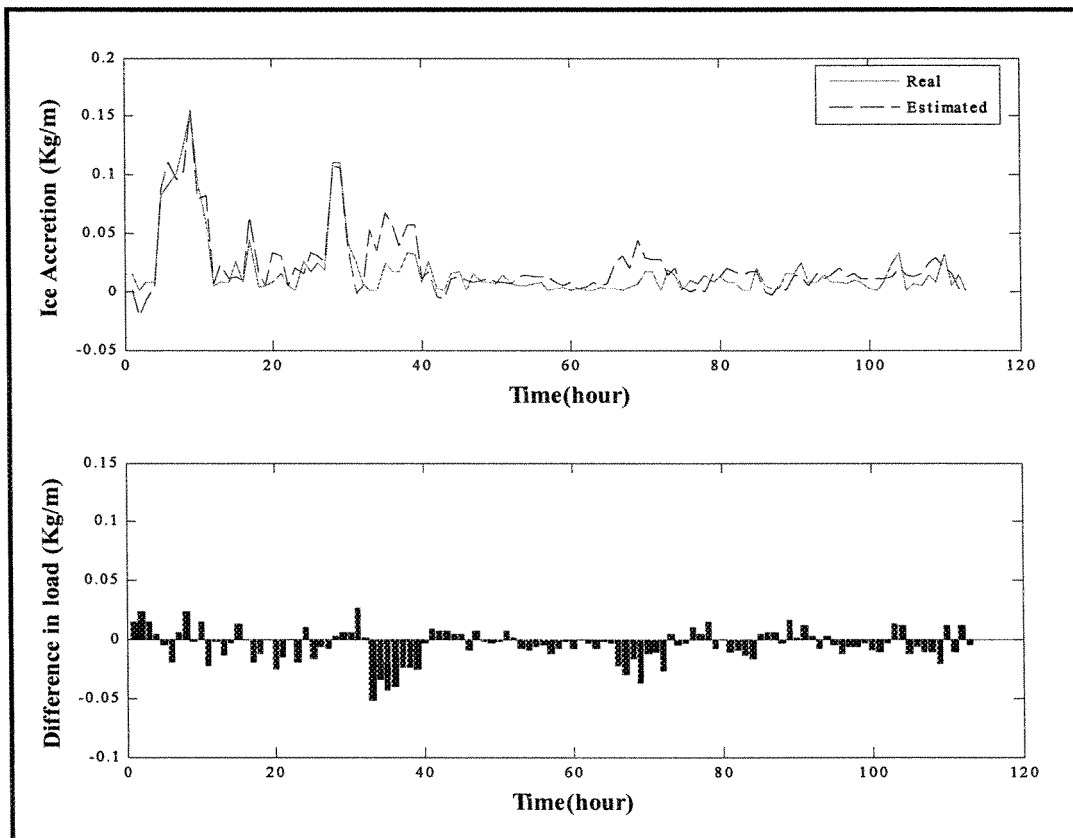
Figure 5-16: "Nowcasting" results of the optimum structure of Jordan with test data set (top), Error bar (bottom)

By comparing the above curves, one can notice that none of the architectures is capable of a perfect estimation of icing rate, and with all the architectures there are errors between the output of the neural network and the measured icing rate. However, with Jordan architecture, the maximum error is less than 0.05 kg/m/h, while with other architectures, the error reaches 0.15 kg/m/h. These curves also lead to the same

conclusion: that Jordan architecture is the most appropriate architecture for estimations of icing rate.

5.6 Predictive models

The ultimate aim of the initial experiments was to provide the basis for developing a model for prediction tasks. We repeat that the learning task in initial experiments was curve fitting with the aim of finding the mapping between the input and output. However, the issue of prediction, which is one of the most pervasive learning tasks, is to predict the present output given a set of some past input patterns. Prediction may be viewed as a form of model building in that the smaller we make the prediction error in a statistical sense, the better the network will serve as a physical model of the underlying process. In mathematical terms, the prediction task of our problem can be represented as:

$$\hat{I}(t) = F\left(\begin{matrix} T(t-1), T(t-2), ..., T(t-M) \\ W(t-1), W(t-2), ..., W(t-M) \\ P(t-1), P(t-2), ..., P(t-M) \\ Z(t-1), Z(t-2), ..., Z(t-M) \\ S(t-1), S(t-2), ..., S(t-M) \end{matrix}\right) \qquad \text{5-2}$$

where $\hat{I}$ is the predicted ice accretion rate at time t, T is the temperature variable, W is the wind velocity, P is the precipitation rate, Z is the wind direction, S is the number of IRM signals, and (t-n) n=1:M refer to the past values of the parameters up to M previous hours.

In the context of this study, because of the limitation in the data size, M was limited to 3 and only up to three previous hours have been used for building the one hour ahead predictive models. For each of the data bases including "accretion phase", "complete event" and "precipitation event", three types of predictive models using the four optimum structures achieved by the initial experimenters were tested. In the first type, the values of the input parameters in time t-1 are presented to the network and it is trained to predict the value of ice accretion at time t. In this case, the number of inputs to the network is five, as with the curve fitting mode. In the second predictive model, the previous values of the input parameters in time t-1 and t-2 are represented to the network and the number of the inputs to the network is ten. Similarly, in the third predictive mode, the past values of input parameters in the three previous hours are represented to the network and the number of the network inputs is fifteen.

5.6.1 Results of predictive models based on NMSE

In this section, the results of experiments based on NMSE are presented. For each data set, three different types of predictive models by variation of the number of inputs taken from previous time steps were tested. All the tests were carried out using the optimum configurations for each of the architectures achieved from the initial experiments.
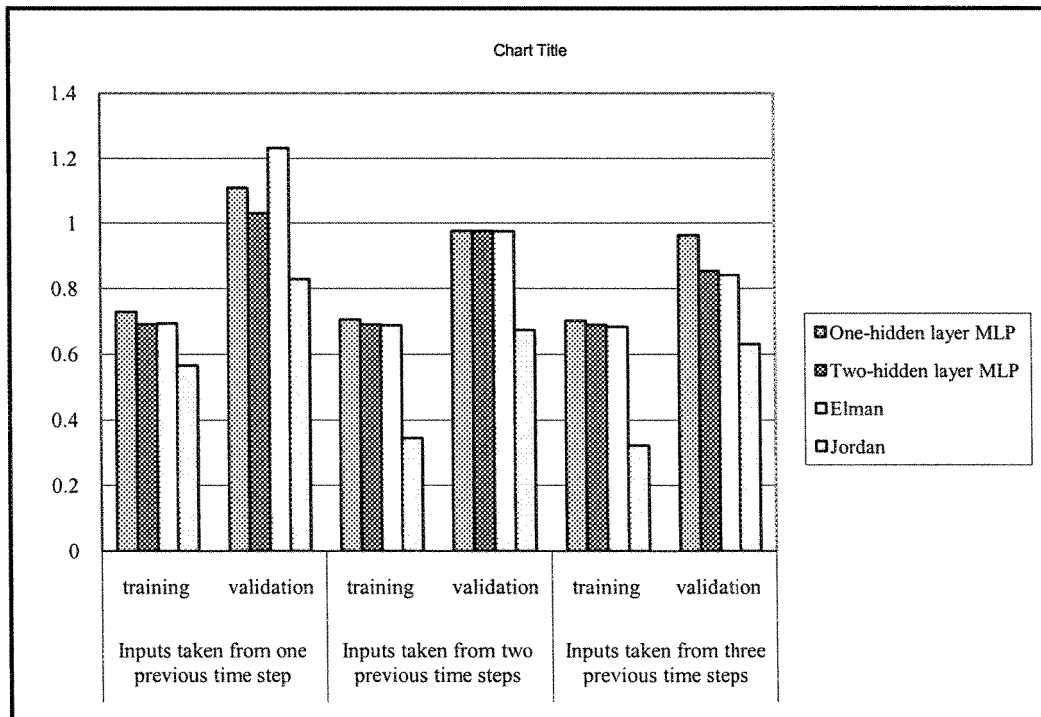
Figure 5-17: Results of three predictive models with four architectures using different past inputs for "Complete event" data base
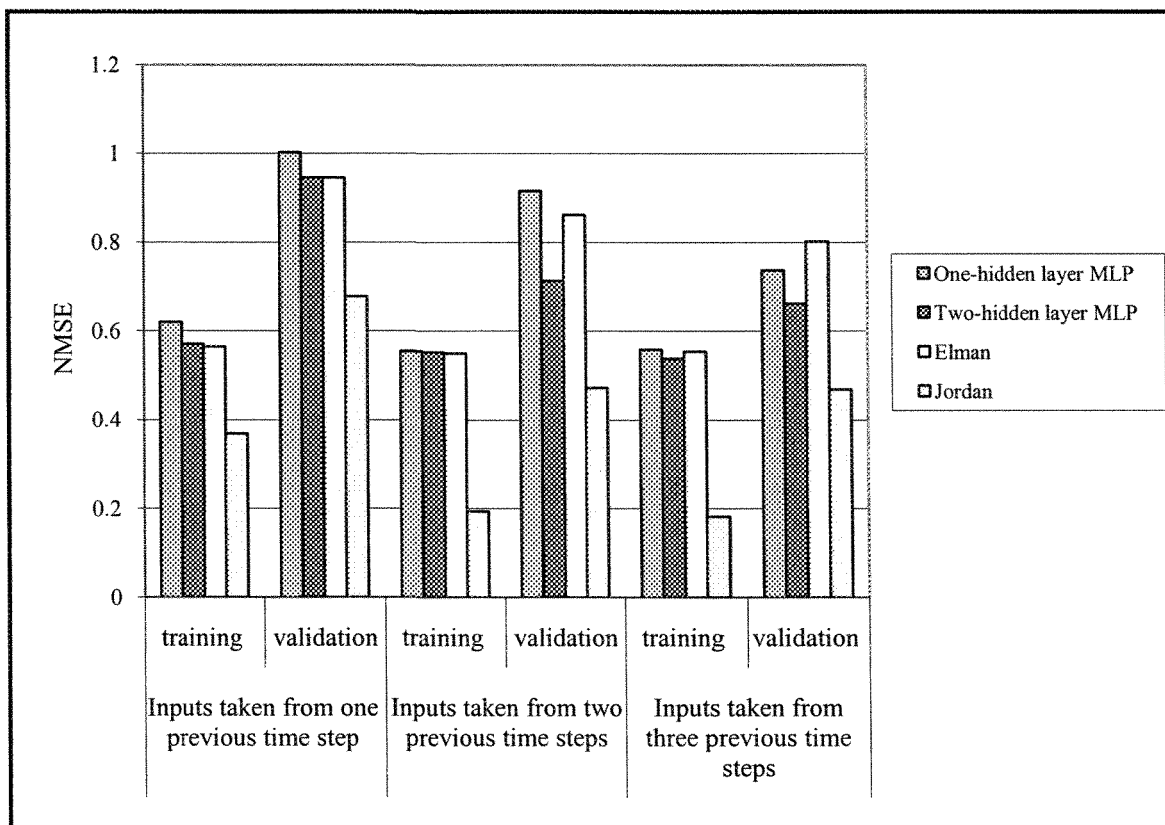
Figure 5-18: Results of three predictive models with four architectures using different past inputs for "Precipitation event" data
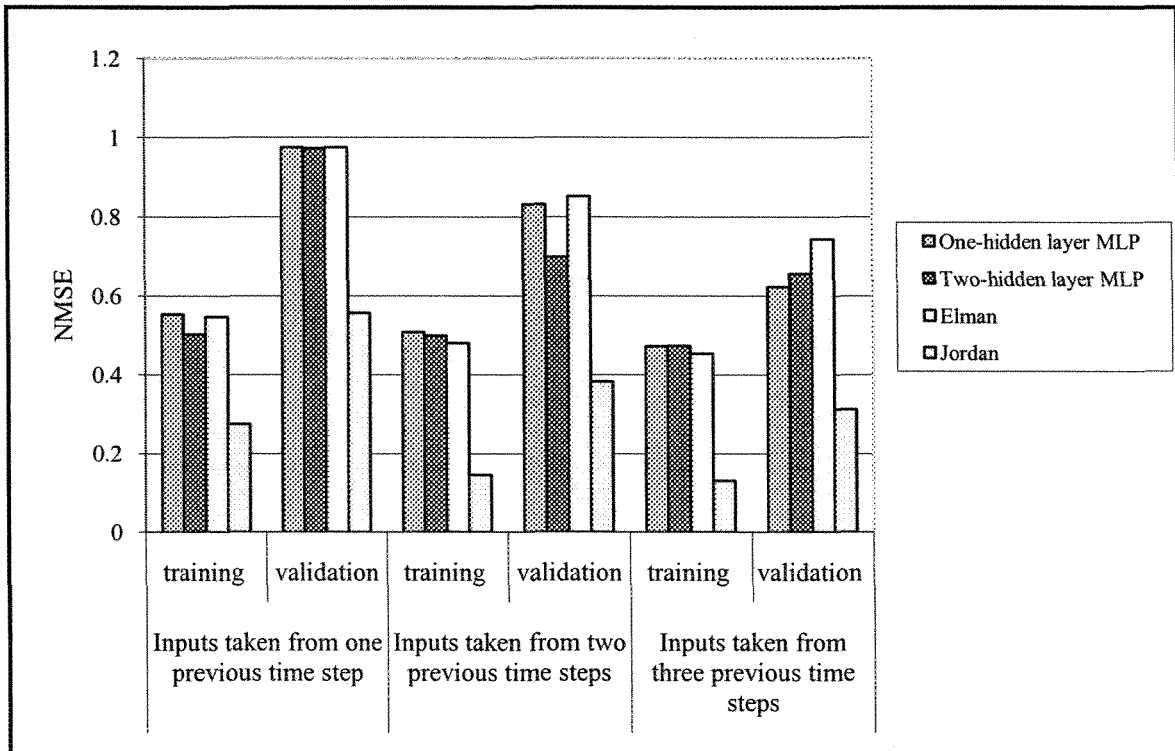
Figure 5-19: Results of three predictive models with four architectures using different past inputs for "Accretion phase" data

From Figures 4-17 to 4-18, it can be observed that augmenting the number of inputs taken from past previous hours increases the predictive efficiency of the neural networks and this is true for all four architectures with all databases. Also, as with the results obtained in the initial experiments, Jordan's architecture gives the best results compared to the other architectures. In the case of comparison of the results obtained with the three databases, it is evident that the more a database becomes homogenous, the better the results. Therefore, the "accretion phase" database is the one which gives the best results. After that, the "precipitation event" data base gives results which are not very satisfactory but better than those obtained by considering the whole data base without any discrimination (as in the "complete event" data). Based on these results, it can be

concluded that Jordan's architecture, with 30 neurons in the hidden layer and using three previous values of the input parameters, is the best candidate for building a predictive model to forecast ice accretion rate. The following figure shows the schematic of this predictive model.
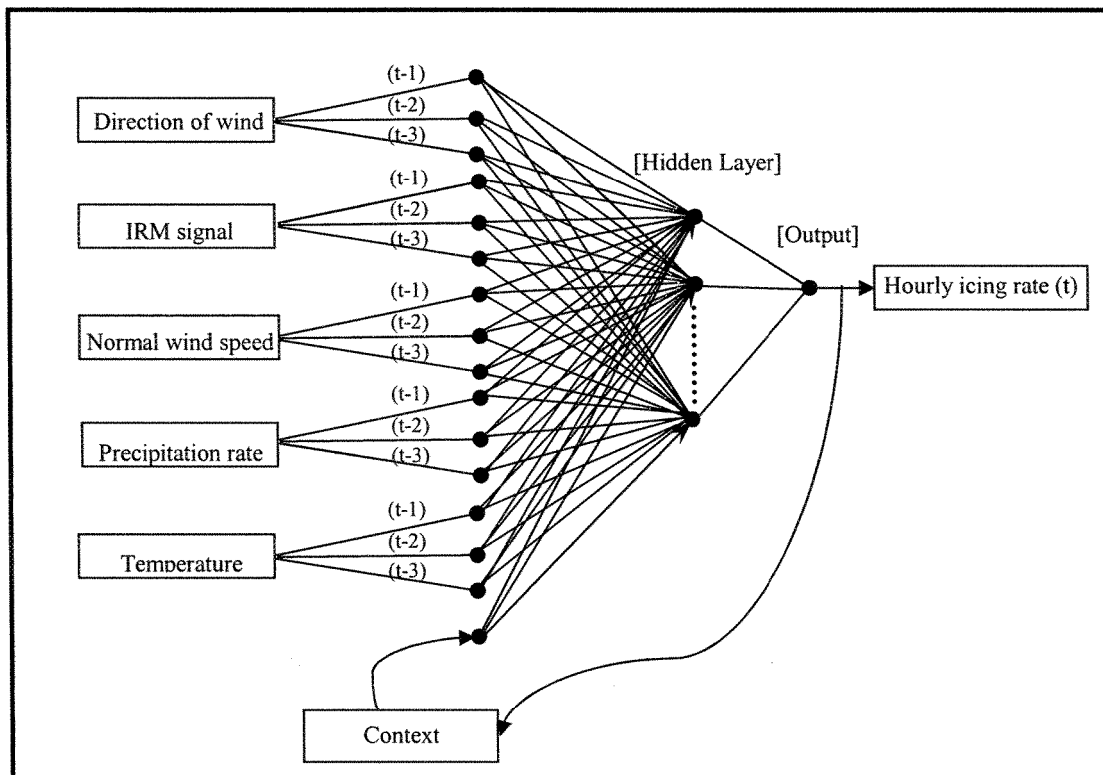
Figure 5-20: Schematic of the finalized predictive model (Jordan's network with fifteen inputs and thirty neurons in the hidden layer)

5.6.2 Prediction curves of the optimum predictive neural network models

As seen in the previous section, Jordan's architecture with the inputs taken from three previous time steps gives the best results for all three databases. Here, the prediction results of this architecture with three test data sets are represented. The following figure shows the prediction results of this architecture for a "complete event" test data set. For the majority of points, the error between the estimated ice load and the real one is less than 0.05 but there are some points for which the error reaches 0.1. For these specific points, it is possible that the test data is out of the training range for some input variables.
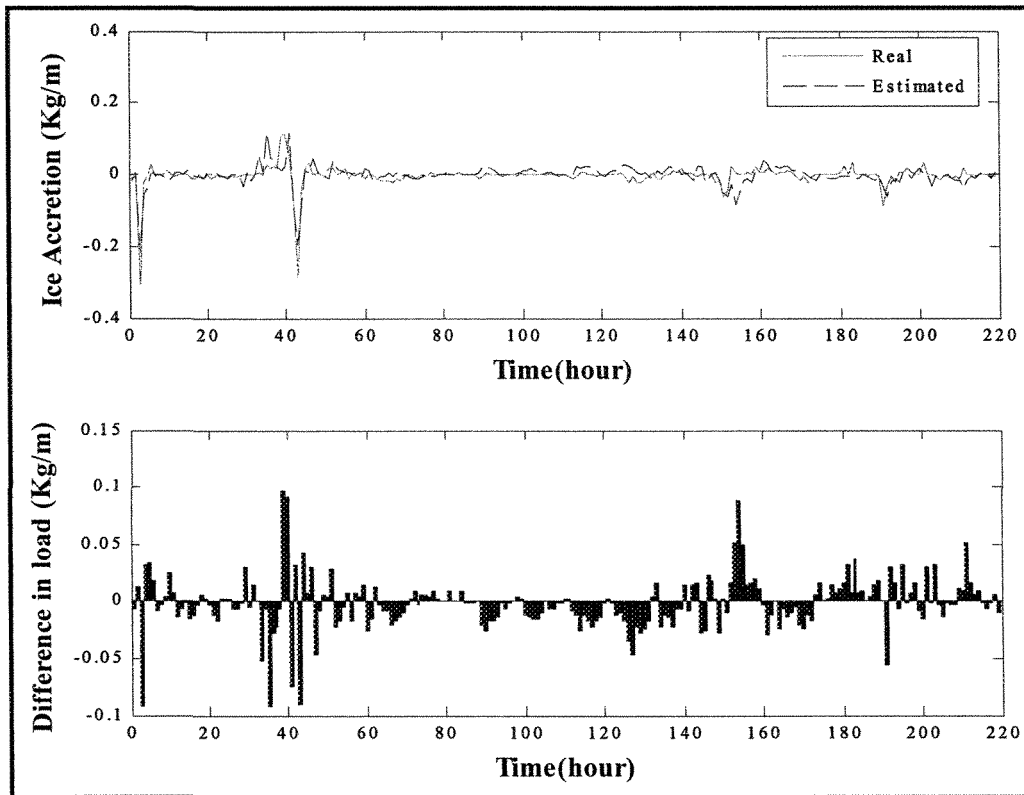
Figure 5-21: Predictive results of the Jordan's predictive neural network model with 15 inputs taken from three previous time steps for the "Complete events" data base (top), Error bar (bottom)

Figure 5-22 shows the prediction results of Jordan's predictive model for a "precipitation events" test data set. For the majority of points, the error between the estimated ice load and the real one is less than 0.05 but there are some points for which the error reaches 0.1. Although this model also gives some important errors, the results are better than for the "complete event" data.
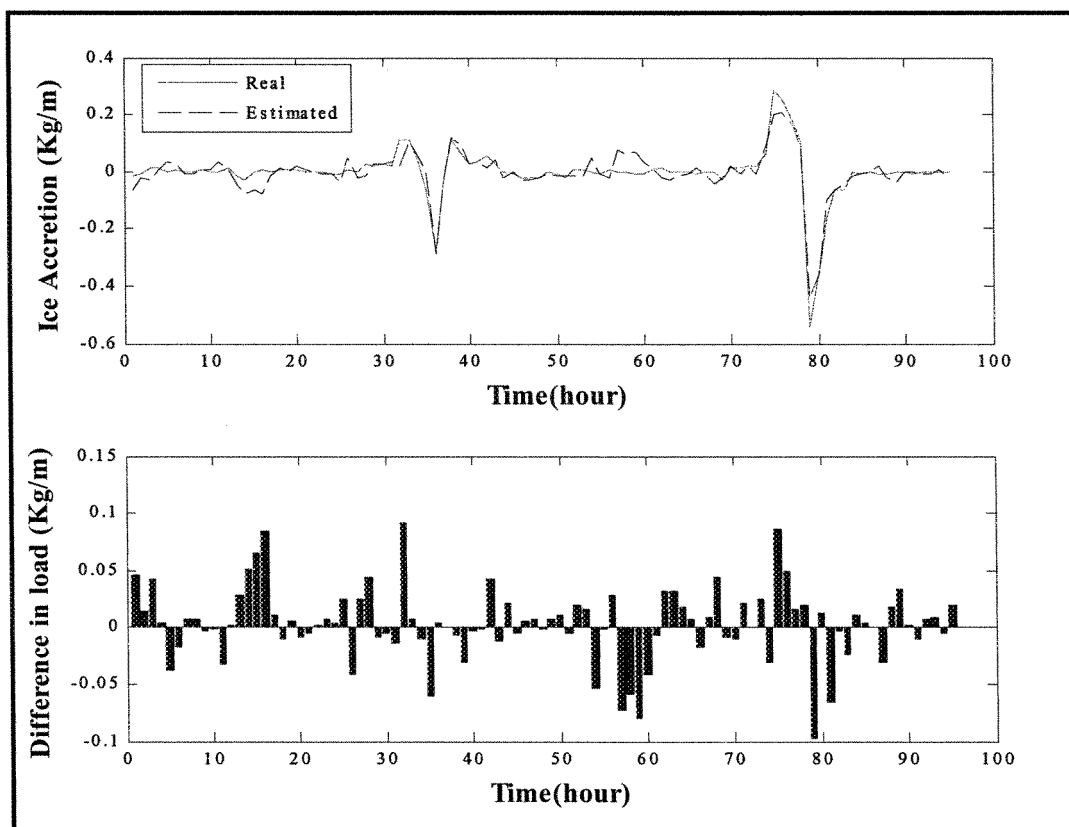
Figure 5-22: Predictive results of the Jordan's predictive neural network model with 15 inputs taken from three previous time steps for the "Precipitation events" data base (top), Error bar (bottom)

Finally, Figure 5-23 shows the prediction results of the optimum predictive model with an "accretion phase" test data set. It can be observed that the errors for all points are less than 0.05 and the model developed for this data set has the best prediction results.

Figure 5-23: Predictive results of the Jordan's predictive neural network model with 15 inputs taken from three previous time steps for an "Accretion phase" data base (top), Error bar (bottom)

The above three curves clearly demonstrate that the homogeneity of the training data for developing neural network models plays an essential role in their proficiency. However, in spite of the good results of the predictive model for the "accretion phase" data 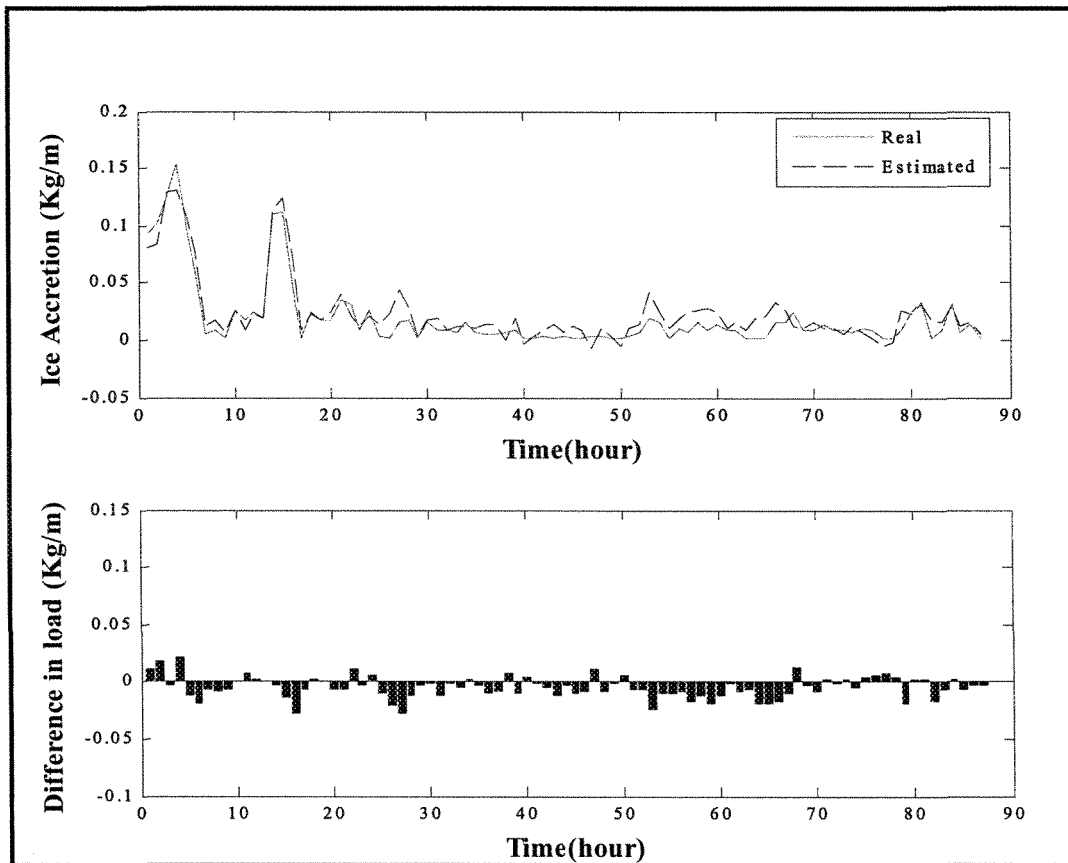set, a perfect prediction was not achieved and this is mainly because of the scarcity of the data volume used in developing the models.

5.7   Summary

In this chapter, three models were developed for predicting the ice accretion rate, each of which is appropriate for a different situation. These models were developed using data from the Mont Bélair measuring station, which is one of the stations of the SYGIVRE data base. In the development of these models, the following approach was taken:

1.   A preliminary analysis of the available database was done in order to determine the input parameters to the network. Based on this preliminary analysis of data, five parameters were selected as the inputs to neural network models for predicting the ice accretion rate on transmission lines. These parameters include temperature, precipitation rate, IRM signals, normal wind speed and direction.

2.   Some initial experiments were done in order to determine the type of the transfer functions used in hidden and output layers. The results showed that using tangent hyperbolic in both layers leads to the best performance.

3.   Four architectures of neural networks were selected to be tested. These include one-hidden layer MLP, two-hidden layer MLP, Elman's and Jordan's

networks. In order to find out which structure of these architectures gave better results, about thirty configurations were tested for each of the structures with variations of the neurons in the hidden layer and in the "nowcasting" mood. This part was the most time-consuming part. The four configurations that gave the best results were selected for developing predictive models.

4. In order to develop predictive models, the neural networks were fed with the past values of the input parameters for predicting the ice accretion rate for the given time. It was observed that increasing the number of inputs taken from past time steps considerably improves the performance of all neural networks. However, because of the limitation in the size of data, only up to three previous time steps were considered.

5. In order to investigate the effect of the filtering data base on the efficiency of the predictive model, three different data bases were extracted from the Mont Bélair data and the results of the experimented predictive models were compared.

Based on these experiments, it was concluded that Jordan's RNN is the best candidate for predicting ice accretion rate. The results showed that increasing the number of previous hours considerably improved the prediction effectiveness of the model. In the context of studying the effect of the data filtering, it was seen that the more homogenous the training data, the better the learning and generalization capacities of neural network models. The best results were achieved by considering only the accretion phase of the

icing events. Consequently, the model developed for the accretion phase data yielded the best results. In spite of the reasonable results obtained with these predictive models, and especially with the model for the "accretion phase" data set, using these predictive models in the real world involves, however, doing the training with much more data. Fortunately, the neural network approach to ice accretion modeling has the advantage of adapting the model to new data as they become available, and the training can be made repeatedly. Therefore, it will be possible to achieve an accurate empirical model for estimating power transmission line icing loads by using the proposed Jordan's architecture as well as a reasonable number of ice data.

Chapter 6

Conclusions and Recommendations

Chapter 6

Conclusions and Recommendations

6.1 Conclusions

The development of neural network-based empirical models for predicting hourly ice accretion rate on transmission lines and predicting accreted ice type on exposed structures has been addressed in this Master's study. Different characteristics of the neural networks were tested in order to determine an appropriate design for each model. The concluding remarks are subdivided in two parts:

6.1.1 Predicting accreted ice type

✓ A two-input neural network model was developed to determine the type of accreted ice using ambient temperature and wind speed. A training data set was created based on the functions extracted from [25]. A one-hidden layer perceptron with 10 neurons in the hidden layer and with logistic sigmoid functions in both hidden and output layers had the best performance. The proposed model has a good prediction of 100% with the training data set and more than 99% with a test data set. The test data set was the icing data recorded at the Mont Bélair station.

✓ A three-input neural network model was developed to determine the type of accreted in-cloud ice, using ambient temperature, wind speed, and droplet size. The training data set was created based on the functions extracted from [11]. A one-hidden layer perceptron with 14 neurons in the hidden layer and with

logistic sigmoid functions in both hidden and output layers had the best performance. The proposed model has a performance of nearly 100% with the training data set.

It should be noted that the accuracy of these two models is dependent on the accuracy of the references used for creating the training data sets and the models are valid and reliable as long as the references used for creating training data sets are valid.

6.1.2 Predicting hourly ice rate

✓ Based on the preliminary analysis of data, five parameters were selected as the inputs to neural network models for predicting ice accretion rate on transmission lines. These parameters include temperature, precipitation rate, IRM signals, normal wind speed and direction.

✓ In developing predictive models, it was concluded that increasing the number of inputs taken from past time steps considerably improves the performance of all neural networks. However, because of the limitation in the size of the data, only up to three previous time steps were considered.

✓ Among four experimented architectures (one-hidden layer MLP, two- hidden layer MLP, Elman and Jordan), Jordan's time-dependent network with 30 neurons in the hidden layer gave the best results with both the training and validation data sets.

✓ Three predictive models were developed, each of which is appropriate for different situations. The first model was developed only with ice accretion data.

The second one was developed by considering all the phases of an icing event. The last one was developed for precipitation events.

✓ The comparison between different predictive models demonstrates that the more homogenous the training data, the better the learning and generalization capacity of neural network models. Consequently, the model developed for the accretion phase data yielded the best results.

In spite of the vast number of different configurations and possibilities that were tested during this study and despite major improvements compared to the previous research work of this kind, an exact prediction was not achieved by any of the three predictive models, mainly because of the limitation in the data size used in training the neural networks. In fact, one of the most important components in the success of any neural network solution is the data. The quality, availability, reliability, and repeatability of the data used to develop and run the system is critical to its success. Unfortunately, the size of the data used in this study was very limited and there were no means for verifying its quality. This problem limits us in generalizing our conclusions. Despite that, however, the results of this study clearly show that it is possible to have a good predictive neural network model provided that all possible configurations are tested and a reasonable number of data is used.

6.2 Recommendations

- In this study a model was devised for determining accreted in-cloud ice type using three parameters (ambient temperature, wind speed, and droplet size). However, because of the lack of the droplet size variable in the databases of SYGIVRE, we couldn't validate this model. Therefore, validation of this model on a database including these parameters is suggested.

- It would be interesting to validate the developed models for predicting ice accretion using different data, for example, using databases from external sources, such as other stations of the SYGIVRE database.

- It is suggested to carry out other experiments for improving the achieved ice accretion predictive models by providing the neural networks with at least ten years' worth of data from all stations in the SYGIVRE network. Also, it would be better if the measurements of stations in the periods out of icing events were to be integrated in the training data. This would create a separation gap between icing events and help neural networks generalize better for each specific icing event.

- It is also suggested to develop ice accretion models by combining the neural network and Fuzzy Logic. Fuzzy Logic could do the data filtering automatically.

References

[1] Ben Kröse, Patrick, V.D. Smagt., *"An Introduction to Neural Network."* The University of Amsterdam, 1996

[2] Boyer, A. E. and Meale, J. R., "Insulation Flashover under Icing Conditions on the Ontario-Hydro 500 kV Transmission Line System" Proceedings of CEA Spring Meeting, Montreal, Canada, March 1988.

[3] Caudill, M. and Butler, C. "Naturally Intelligent Systems." 1990, Cambridge, Mass: MIT Press.

[4] Chainé, P.M. and Castonguay, G., "New Approach to Radial Ice Thickness Concept Applied to Bundle-like Conductors". Industrial Meteorology-Study IV, Environment Canada, Toronto, 1974, 11.p.

[5] Chen, Y., "A 2-D Random Walk Model for Predicting Ice Accretion on a Cylindrical Conductor", Master's Degree Thesis, UQAC, 2001.

[6] Chen, Y., Farzaneh, M., Lozowski, E.P. and Szilder, K., "Modeling of Ice Accretion on Transmission Line Conductors", Proceedings of the 9th International Workshop on Atmospheric Icing of Structures, Chester, United Kingdom, June 2000, Session 7a, 8.p.

[7] Chester, M., "Neural Networks, A Tutorial", Prentice Hall, Englewood Cliffs, NJ, 1993

[8] Chouinard, L.E., Elfashny, K.N.G, Nguyen, V.T.V. and Laflamme, J., "Modeling of Icing Events Based on Passive Ice Meter Observations in Quebec". Atmospheric Research 46, Elsevier, 1998, pp. 169-179.

[9]   Daniel T.Larose. "Une Introduction au Data Mining", Traduction et adaptation de Thierry Vallaud

[10] Duda, Richard O., Stork, David G. and Hart, Peter E., "Pattern classification" , New York, Toronto: Wiley, c2001

[11] Electric Power Research Institute. Transmission Line Reference Book: Wind-Induced Conductor Motion, EPRI Research Project 792, Palo Alto, CA, USA, 1979.

[12] Elfashny, K.N.G., Nguyen, V.T.V., Chouinard, L.E. and Laflamme, J.N., "Statistical Analysis of Ice Observations in Quebec, Canada". 8th International Workshop on Atmospheric Icing of Structures. Reykjavik, Iceland, 1998, pp.273-278.

[13] Elman, J., "Finding Structure in Time", Cognitive Science 14, 1990, pp.179-211.

[14] Environment Canada http://www.msc-smc.ec.gc.ca/media/icestorm98/

[15] Eter, W., Houde, L. and Farzaneh, M., "Système de suivi des tempêtes de verglas en   temps réel.", 2003.

[16] Farzaneh, M., "Ice Accretion on H.V. Conductors and Insulators and Related Phenomena". Invited article, Philosophical Transactions, The Royal Society, London, No. 358, 2000, pp. 1-35.

[17] Farzaneh, M. and Savadjiev, K., "Icing Events Occurrence in Quebec: Statistical Analysis of Field Data". Proceedings of the 8th International Offshore and Polar Engineering. Montréal (QC), Canada, 1998

[18] Farzaneh, M. and Savadjiev, K., "Statistical Analysis of Field Data for Precipitation Icing Accretion on Overhead Power lines". IEEE Transactions on Power Delivery, Vol.20, No.2, 2005

[19] Fortin.R, Laflamme.J and Coté.Y, "SYGIVRE, the Hydro-Quebec Real Time Icing Events Management System", 7th International Workshop on Atmospheric Icing of Structures. Chicoutimi (QC), Canada, 1996,.p. 459

[20] Gates, E.M., Liu, A. and Lozowski, E.P., "A Stochastic Model of Atmospheric Rime Icing". J. Glaciol., Vol. 34 No. 12, 1988, pp. 26-30.

[21] Guesdon, C., Houde, L., Farzaneh, M. and Chouinard, L., " Études des répartitions des evènements de verglas et de givre à travers le Québec", Université du Québec à Chicoutimi., 2000.

[22] Haykin, S. "Neural Networks-A Comprehensive Foundation", Prentice-Hall, New York, 1999.

[23] Hopfield, J., "Neural Networks and Physical Systems with Emergent Collective Computational Properties," Proc. National Academy of Science of the USA, vol.79, 1982, pp. 2554-2588.

[24] Houde, L., Guesdon, C., Farzaneh, M. and Chouinard L., "Analysis of Spatial Patterns for Icing Events in Quebec". 9th International Workshop on Atmospheric Icing of Structures. Chester, United Kingdom, 2000, session 2, 8p.

[25] IEC (CEI) 60826 (Third edition, 2003). "Design Criteria of Overhead Transmission Lines".

[26] Imai, I. "Studies on Ice Accretion". Researches on Snow and Ice, No. 1,1953, pp. 35-44

[27] José, C.Principe, Neil, R.Euliano and W.Curt Lefebvre. "Neural and Adaptive Systems"

[28] Kannus, K. and Verkkonen, V., "Effect of Coating on the Dielectric Strength on High Voltage Insulators", Proceeding of 4th International Workshop on the Atmospheric Icing of Structures, Paris, France, 1988, pp. 296-300.

[29] Laflamme, J., "Spatial Variation of Extreme Values in the Case of Freezing Rain Icing". 6th International Workshop on the Atmospheric Icing of Structures. Budapest, Hungray, 1993, pp.19-23.

[30] Laflamme, J. and Périard, G., "The Climate of Freezing Rain over the Province of Quebec in Canada: A Preliminary Analysis". 7th International Workshop on Atmospheric Icing of Structures. Chicoutimi (QC), Canada, 1996, pp.19-24.

[31] Laflamme.J, Latour.A and Côté, Y., "Description of the Mont Bélair Ice Load Measurements Site", 7th International Workshop on Atmospheric Icing of Structures. Chicoutimi (QC), Canada, 1996, .p. 453

[32] Langmuir, I. and Blogett, K.B., "A Mathematical Investigation of Water Droplet Trajectories". U.S.A. Air Force Technical Report No. 5418, 1946, 65.p.

[33] Larouche, E., Rouat, J., Bouchard, G. and Farzaneh, M., "Exploration of Static and Time Dependent Neural Network Technique for the Prediction of Ice Accretion on Overhead Line Conductors". 9th International Workshop on Atmospheric Icing of Structures. Chester, United Kingdom, 2000.session 2, 8.p.

[34] Lenhard, R.W., "An Indirect Method for Estimating the Weight of Glaze on Wires". Bull. Amer. Meteor. Soc, Vol. 36, 1955, pp. 1-5.

[35] Li, Y., "Étude de l'influence de l'altitude sur les caractéristiques de l'arc électrique à la surface de glace polluée" Thesis of Ph.D. in Engineering, UQAC, 2002.

[36] Lu, MX., Olivier, P., Popplewell, N. and Shah, A.H. "Predicting Extreme Loads on a Power Line from Freezing Rainstorms". 9th International Offshore and Polar Engineering Conference. Brest, France, 1999, pp.594-598.

[37] Makkonen, L., "Modeling Power Line Icing in Freezing Precipitation". 7th International Workshop on Atmospheric Icing of Structures, Chicoutimi, Canada, 1996, pp. 195-200.

[38] Makkonen, L. and Stallabrass, J. R., "Ice Accretion on Cylinders and Wires" National Research Council of Canada, Low Temperature Laboratory, 175 Report TR-LT-005,1984.

[39] Marzban, C. and Stumpf, G., "A Neural Network for Tornado Prediction Based on Doppler Radar-Derived Attributes". *Journal of Applied Meteorology,* 35, 1996,pp.617-626

[40] McComber, P., De lafontaine, J., Druez, J., Laflamme, J. and Paradis, A. "A Comparison of Neural Network And Multiple Regression Tranmission Line Icing Models. " Proceedings of 55th Eastern Snow Conf., Jackson, NH, 1998.

[41] McComber, P., de Lafontaine, J. and Laflamme, J., "A Neural System to Estimate Transmission Line Icing". 8th International Workshop on Atmospheric Icing of Structures, Reykjavik, Iceland, 1998, pp. 101-106.

[42] McComber, P., Druez, J. and Laflamme, J. "Icing Rate Estimation of Atmospheric Cable Icing". Int. J. Offshore & Polar Eng. Vol.5, No.2, 1995, pp.75-92.

[43] McComber, P., Latour A., Druez J. and Laflamme J., "The Icing Rate Meter, an Instrument to Evaluate Transmission Line Icing". 7th International Workshop on Atmospheric Icing of Structures. Chicoutimi (QC), Canada, 1996, pp.159-168.

[44] McCulloch, W. and Pitts, W. "A Logical Calculus of the Ideas Immanent in Nervous Activity." Bulletin of Mathematical Biophysics. 7, 1943, pp. 115-133.

[45] Minsky, M., and Seymour, P., "Perceptrons: An introduction to Computational Geometry", 1969, MIT Press.

[46] Ohta, H., Saitoh, K., Kanemaru, K., Ijichi, Y. and Kitagawa, H., "Application of Disaster Warning System Due to Snow Accretion on Power Lines Using Neural Networks". 7th International Workshop on Atmospheric Icing of Structures, Chicoutimi, Canada, 1996, pp149-154.

[47] Personne, P., Curoure, C. and Isaka, H., "Theoretical Study of Air Inclusion on Rotating Cylinders". 5th International Workshop on Atmospheric Icing of Structures, Tokyo, Japan, 1990, pp. A2-6.

[48] Poots, G., "Ice and Snow Accretion on Structures" Research Studies Press LTD, 1996.

[49] Rosenblatt, F., "The Perceptron: A Probabilistic Model for Information Storage and Organization in the Brain.", Cornell Aeronautical Laboratory, *Psychological Review*, Vol.65, No. 6, 1958, pp. 386-408.

[50] Savadjiev, K. and Farzaneh, M., "Statistical Analysis of Two Probabilistic Models of Ice Accretion on Overhead Line Conductors". Proceedings of 8th International Offshore and Polar Engineering. Montréal (QC), Canada, 1998, 9.p.

[51] Savadjiev, K., Farzaneh, M. and Druez, J., "Analysis and Interpretation of Icing Rate Meter and Load Cell Measurements on the Mt. Blair Icing Site". Proceedings of 9th International Offshore and Polar Engineering. Brest, France, pp.607-611, 1999.

[52] Savadjiev, K., Farzaneh, M. and Druez, J., "Probabilistic Study of Icing and Ice-Shedding on the Mont Bélair Icing Site". Proceedings of 9th International Workshop on Atmospheric Icing of Structures, 2000, 8.p.

[53] Savadjiev, K., Farzaneh, M. and Druez, J., "Study of Icing Rate and Related Meteorological Parameter Distributions during Atmospheric Icing Events". Proceedings of 11th International Offshore and Polar Engineering. Stavanger, Norway, 2001, pp.665-670.

[54] Savadjiev, K., Latour, A. and Paradis, A., "Estimation of Ice Accretion Weight from Field Data Obtained on Overhead Transmission Line Cables". Proceedings of 7th International Workshop on Atmospheric Icing of Structures. Chicoutimi (QC), Canada, 1996, pp.125-130

[55] Stallabrass, J.R. and Hearty, P.F., "The Icing of Cylinders in Conditions of Simulated Freezing Sea Spray". National Research Council of Canada, DME Report MD-50, 1967, 15.p.

[56] Szilder, K., "Simulation of Ice Accretion on a Cylinder Due to Freezing Rain." *JGlaciol,* Vol. 40, No. 136, 1994, pp.586-594.

[57] Szilder, K., "The Density and Structure of Ice Accretion Predicted by a Random-Walk Model" Quart. J. Roy. Meteor. Soc, Vol. 119, No. 513, 1993, pp. 907-924.

[58] Szilder, K. and Lozowski, E.P., "Morphogenetic Modeling of Wet Ice Accretions on Transmission Lines as a Result of Freezing Rain" Proceedings of the 9th International Offshore Polar Engineering Conference, *ISOPE,* Brest, Vol. II, 1999, pp. 616-621.

[59] Szilder, K. and Lozowski, E.P., "Simulation of Icicle Growth Using a Three-Dimensional Random Walk Model *Atmospheric Research*." Vol. 36, No. 1, 1995, pp. 243- 249.

[60] Welstead, S.T., *"Neural Network and Fuzzy Logic Applications in C++",* John Wiley & Sons, Inc., 1994

[61] Widrow,B. and M.E.Hoff., "Adaptive Switching Circuits." IRE WESCON Convention Record, 1960,pp.96-104